Gravitational dynamics of an infinite shuffled lattice of particles

T. Baertschiger
Dipartimento di Fisica, Università "La Sapienza," Piazzale A. Moro 2, I-00185 Rome, Italy and Istituto dei Sistemi Complessi–CNR, Via dei Taurini 19, I-00185 Rome, Italy

M. Joyce
Laboratoire de Physique Nucléaire et de Hautes Energies, Université Pierre et Marie Curie-Paris 6, UMR 7585, Paris, F-75005 France

A. Gabrielli
ISC-CNR, Via dei Taurini 19, I-00185 Rome, Italy, and SMC-INFM, Dipartimento di Fisica, Università "La Sapienza", Piazzale A. Moro 2, I-00185 Rome, Italy

F. Sylos Labini
"E. Fermi" Center, Via Panisperna 89 A, Compendio del Viminale, I-00184 Rome, Italy and Istituto dei Sistemi Complessi–CNR, Via dei Taurini 19, I-00185 Rome, Italy

(Received 15 July 2006; published 15 February 2007)

We study, using numerical simulations, the dynamical evolution of self-gravitating point particles in static Euclidean space, starting from a simple class of infinite "shuffled lattice" initial conditions. These are obtained by applying independently to each particle on an infinite perfect lattice a small random displacement, and are characterized by a power spectrum (structure factor) of density fluctuations which is quadratic in the wave number k, at small k. For a specified form of the probability distribution function of the "shuffling" applied to each particle, and zero initial velocities, these initial configurations are characterized by a single relevant parameter: the variance δ^2 of the "shuffling" normalized in units of the lattice spacing ℓ. The clustering, which develops in time starting from scales around ℓ, is qualitatively very similar to that seen in cosmological simulations, which begin from lattices with applied correlated displacements and incorporate an expanding spatial background. From very soon after the formation of the first nonlinear structures, a spatiotemporal scaling relation describes well the evolution of the two-point correlations. At larger times the dynamics of these correlations converges to what is termed "self-similar" evolution in cosmology, in which the time dependence in the scaling relation is specified entirely by that of the linearized fluid theory. Comparing simulations with different δ, different resolution, but identical large scale fluctuations, we are able to identify and study features of the dynamics of the system in the transient phase leading to this behavior. In this phase, the discrete nature of the system explicitly plays an essential role.

DOI: 10.1103/PhysRevE.75.021113 PACS number(s): 05.20.−y, 95.30.Sf

I. INTRODUCTION

The problem of the evolution of self-gravitating classical particles, initially distributed very uniformly in infinite space, is as old as Newton. Modern cosmology poses essentially the same problem as the matter in the universe is now believed to consist predominantly of almost purely self-gravitating particles—so-called dark matter—which is, at early times, indeed very close to uniformly distributed in the universe, and at densities at which quantum effects are completely negligible. Despite the age of the problem and the impressive advances of modern cosmology in recent years, our understanding of it remains, however, very incomplete. In its essentials, i.e., stripped of the full detail of current cosmological models, it is a simple well-posed problem of out of equilibrium statistical mechanics[1]. In this context, however, it has been relatively neglected, primarily because of the intrinsic difficulties associated with the attractive long-range nature of gravity and its singular behavior at vanishing separation. In recent years there has, however, been renewed interest (see, e.g., [2]) in the physics of systems with long-range interactions, in which context self-gravitating systems are one of the paradigmatic examples (for a review, see, e.g., [3]). A considerable amount of work on these systems in this context has focused on *finite* systems (see, e.g., [4–7])—in which, in certain cases, some of the instruments of equilibrium statistical mechanics may be applied[2]—and on more

[1]Strictly speaking it is not actually known whether the problem is well-controlled without a regularization of the singularity in the gravitational force at $r=0$ (see, e.g., [1] for a recent discussion and list of references). In practice, in numerical simulation, there is no intrinsic problem in implementing the N-body gravitational dynamics without such a regularization for typical initial conditions (i.e., in which particles are not placed initially at the same point). In the numerical simulations reported here, as in cosmological simulations, we do, however, use such a regularization. This is done solely for numerical efficiency, and the results analyzed are tested numerically for their independence of the associated cutoff (see below).

[2]We note that in [8,9] a treatment of infinite self-gravitating systems in the framework of equilibrium statistical mechanics is developed by considering a "dilute" infinite volume limit, in which $N\to\infty$ and $V\to\infty$ at $N/V^{1/3}$=constant, where N is the number of

tractable one-dimensional models (see, e.g., [11–15]). In cosmology perturbative approaches to the problem, which treat the very limited range of low to modest amplitude deviations from uniformity, have been developed (see, e.g., [16,17]), but numerical simulations are essentially the only instrument beyond this regime. While such simulations constitute a very powerful and essential tool, they lack the valuable guidance which a fuller analytic understanding of the problem would provide. The dynamics of infinite self-gravitating systems is thus both a fascinating theoretical problem of out of equilibrium statistical mechanics, directly relevant both in the context of cosmology and, more generally, in the physics of systems with long-range interactions.

Approaching the problem in the context of statistical mechanics, as we do here, it is natural to start by reducing as much as possible the complexity of the analagous cosmological problem. We wish to focus on the essential aspects of the problem. Thus we consider clustering without the expansion of the universe, and starting from particularly simple initial conditions. With respect to the motivation from cosmology, there is of course a risk: in simplifying we may lose some essential elements which change the nature of gravitational clustering. Our results suggest that this is not the case. Even if it were, it seems unlikely that we will not learn something about the more complex cosmological problem in addressing this slightly different problem.

Gravitational clustering in an infinite space—static or expanding—starting from quasiuniform initial conditions, is intrinsically a problem out of equilibrium. By "quasiuniform" initial conditions we mean that the initial state is a particle distribution—specified, we will assume, by a stochastic point process [18]—which has relative fluctuations at all scales, of small amplitude above the scale characteristic of the particle "granularity" and decaying at infinitely large scales.[3] One of the most basic results (see, e.g., [16,17] and also the appendices to this paper) about self-gravitating systems, treated in a fluid limit, is that the amplitude of small fluctuations grows monotonically in time, in a way which is independent of the scale. This linearized treatment breaks down at any given scale when the relative fluctuation at the same scale becomes of order unity, signaling the onset of the "nonlinear" phase of gravitational collapse of the mass in regions of the corresponding size. In an infinite space, in which the initial fluctuations are nonzero and finite at all scales, the collapse of larger and larger scales will continue *ad infinitum*. The system can, therefore, never reach a time independent state, and in particular it will never reach a thermodynamic equilibrium.[4] One of the important results from numerical simulations of such systems in the context of cosmology is, however, that the system, nevertheless, reaches a kind of scaling regime, in which the temporal evolution is equivalent to a rescaling of the spatial variables [21,22]. This spatiotemporal scaling relation is referred to as "self-similarity."[5] It is observed, however, only starting from a restricted class of simple initial conditions—we will describe these in further detail below—and in the specific Einstein de Sitter (EdS) expanding universe [16]. The range of initial conditions to which it applies has been a point of discussion in the literature, and theoretical explanations of it typically restrict it to quite a narrow range of such initial conditions, and strictly to the EdS expanding universe. To see whether this kind of simple behavior is reproduced in the system we study, is thus a first point of interest. It is in fact the primary focus of this paper.

One comment needs to be made about the use of a static (Euclidean) space time. The problem of bodies interacting by their mutual Newtonian self-gravity in the infinite volume limit, taken at constant mean density, is in fact ill-defined: the force on a particle depends on how the limit is taken. In order to remove this ambiguity one adds a negative background to cancel the contribution of the mean density—the so-called "Jeans swindle" (see, e.g., [24]). As discussed in [25], this is equivalent to taking the limit symmetrically about each particle on which we calculate the total gravitational force.[6] Then only the fluctuations of the density field generate the gravitational force. In the context of cosmological expanding universe solutions, this "swindle" is unnecessary as the expansion absorbs the effect of the mean density, and the perturbations to the co-moving particle trajectories are indeed sourced only by the fluctuations (see, e.g., [16]). This modification does not necessarily make the gravitational force well defined in general: whether it is well defined depends on the nature of the fluctuations in the density field at large scales. For the case of the shuffled lattice (SL) considered here, we have studied in detail the properties of the gravitational force in [25], and shown the force to be well defined in the presence of the canceling background.

Previous works in the same spirit as this [27–29] have treated primarily the very simplest initial condition one can envisage: Poisson distributed particles with no initial veloc-

particles and V is the volume (see also [10] for a more recent discussion). This is not the physically relevant limit for the problem treated here, as we consider the infinite volume limit taken at constant density, i.e., $N\rightarrow\infty$ and $V\rightarrow\infty$ at $N/V=$constant. In this case, as discussed further below, the system is intrinsically time dependent and never reaches a thermodynamic equilibrium.

[3]It is also implicit in the phrase "quasiuniform initial conditions in infinite space" that, as noted above, the infinite volume limit here is taken at constant particle density, rather than in the "dilute" limit studied in [8,9].

[4]This does, of course, not mean that the instruments of equilbrium statistical mechanics are completely irrelevant. Saslaw (see [19] and references therein) notably has developed a treatment of gravitational clustering in an expanding universe which approximates it as a "quasiequilbrium" in which the thermodynamic variables evolve adiabatically with the expansion of the Universe. Another more formal exploration of the usefulness of some standard equilibrium techniques can be found in [20].

[5]Note that this term is here used in a different sense to that commonly ascribed to it in condensed matter physics. In this context "self-similarity" usually implies that the spatial correlations themselves have invariance properties under rescaling (see, e.g., [23]). This is not necessarily the case in the present context.

[6]See [26] for a very clear discussion of this issue. It is also shown here that addition of the negative backgound is equivalent to regularizing the problem with a cosmological constant.

ity. One of the basic results which has been emphasized in these works is the role of nearest neighbor interactions at early times in forming structures (see also [30]), giving rise to nonlinear density-density correlations which are then observed to be reproduced at larger and larger scales as time evolves. At the same time the effects of amplification at larger scales—described by the fluid limit in which the granular structure of the matter is irrelevant—is observed. When trying to address the basic issue of the relative importance of these mechanisms, one runs into the limits imposed by the simple initial conditions: in a Poisson distribution a single parameter—the particle density, or equivalently mean interparticle distance—controls both the amplitude of fluctuations and the "granularity" of the mass distribution. This limitation is one of the major motivations for the different class of initial conditions we study in this work, developing further some initial analysis of this case in [29]: we consider lattices subjected to small random displacements. In this case there are now two parameters, the interparticle distance ℓ and the amplitude Δ of the shuffling. Given the scale free nature of gravity it is in fact only the dimensionless combination $\delta=\Delta/\ell$ which is physically relevant (while in the case of Poisson initial conditions there is effectively no free adjustable parameter). When the dynamics of the SL is treated in the fluid limit, as we will see, configurations with different δ may also be trivially related. In particular we can consider systems with different δ which have different discreteness properties which are equivalent in terms of their fluid description. This allows us to understand notably the aspects of the evolution of the system which can be accounted for in a description of the dynamics in a fluid limit, and those which require the discreteness of the system to be *explicitly* taken into account. This is an important point as almost all existing analytic results on infinite self-gravitating systems are derived in this former limit.[7] Our initial conditions are similar, but not identical, to those used in cosmological simulations of the formation of structure in the Universe. In this context the initial conditions are usually given by simple cubic lattices, perturbed by *correlated* displacements, with relative displacements between nearest neighbor particles which are small [31]. The displacements are generated in reciprocal space starting from an input power spectrum (PS), i.e., what is usually called the "structure factor" in condensed matter physics, specifying the desired theoretical density fluctuations.

In this paper we describe systematically basic results on gravitational dynamics starting from SL initial conditions. Our principal results are the following:

(i) Evolution from these initial conditions converges, after a sufficient time, to a "self-similar" behavior, in which the two-point correlation function obeys a simple spatiotemporal scaling relation. The time dependence of the scaling (i.e., the quantity analogous to the dynamical exponent in out of equilibrium statistical mechanics) is in good agreement with that inferred from the linearized fluid approximation. This result is a generalization of what has been observed, for "redder" initial PS [$P(k)\sim k^n$ with $n\leqslant 1$], in simulations in an EdS universe [21,22,32].

(ii) Between the time at which the first nonlinear correlations emerge in a given SL and the convergence to this "self-similar" behavior, there is a transient period of significant duration. During this time, the two-point correlation function already approximates well, at the observed nonlinear scales, a spatiotemporal scaling relation, but in which the temporal evolution is faster than the asymptotic evolution. This behavior can be understood as an effect of discreteness, which leads to an initial "lag" of the temporal evolution at small scales.

(iii) Simulations with different particle numbers, but the same large scale fluctuations (as characterized by the PS at small k), converge after a sufficient time, not only to the same functional form of the correlation function (with the self-similar behavior), but to the same amplitude. This is further evidence that it is indeed the common large scale fluctuations alone which determine the amplitudes of the correlations, which are thus independent of the discreteness scale ℓ. At early times, however, we see manifest difference between the systems, typically again characterized as a lag of simulations with larger ℓ (and smaller δ).

(iv) The nonlinear correlations, when they first develop, are very well accounted for solely in terms of two-body correlations. This is naturally explained in terms of the central role of nearest neighbor interaction in the build-up of these first nonlinear correlations.

(v) This two-body phase extends to the time of onset of the spatiotemporal scaling, and thus the asymptotic form of the correlation function is already established to a good approximation at this time. We briefly discuss the significance of this quite surprising finding.

The paper is organized as follows. In the next section we briefly define a SL distribution and introduce the main statistical quantities we use in the analysis and their estimators. We discuss the numerical simulations and their analyses in Sec. III. Finally in Sec. IV we summarize our mains results and conclusions, and briefly discuss some of the many open problems which remain for future investigation.

II. SHUFFLED LATTICES AND STATISTICAL QUANTITIES

We first describe (Sec. II A) the class of initial conditions we study. In Sec. II B we define the statistical quantities we will use to characterize the correlations, and in Sec. II C we specify how we estimate these quantities in our simulations.

A. Definition of a shuffled lattice

We use the term SL to refer to the infinite point distribution obtained by randomly perturbing a perfect cubic lattice: each particle on the lattice, of lattice spacing ℓ, is moved randomly ("shuffled") about its lattice site, each particle *in-*

[7] It is also a question which is very relevant in the context of cosmology, as it concerns the understanding of the discreteness effects in simulations of dark matter, which intrinsically limit their precision. These simulations treat the gravitational clustering of point "macro-particles," which typically correspond to the order of 10^{70} dark matter particles.

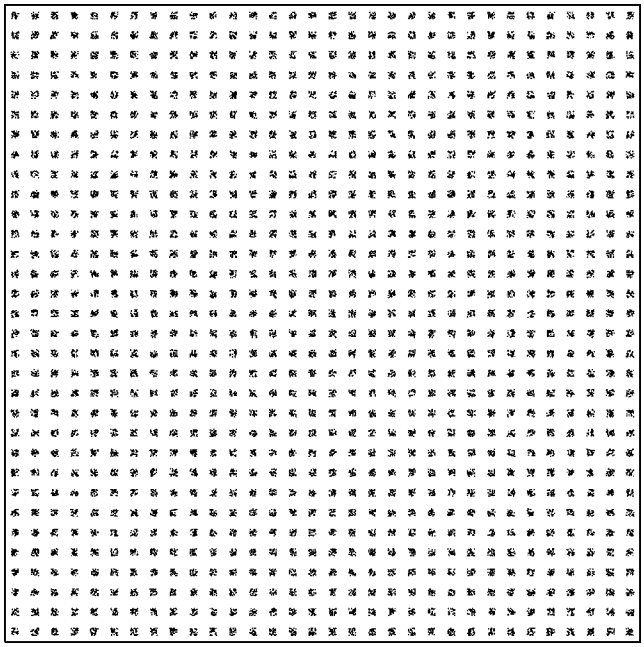

FIG. 1. Projection on the $z=0$ plane of a SL with 32^3 particles and $\delta=0.177$. Due to the random shuffling with the given PDF each lattice "chain" parallel to the z axis projects onto a small square.

dependently of all the others. A particle initially at the lattice site $\mathbf{R}$ is thus at $\mathbf{x}(\mathbf{R})=\mathbf{R}+\mathbf{u}(\mathbf{R})$, where the random vectors $\mathbf{u}(\mathbf{R})$ are specified by the factorized joint probability density function

$$\mathcal{P}[\{\mathbf{u}(\mathbf{R})\}] = \prod_{\mathbf{R}} p(\mathbf{u}(\mathbf{R})). \tag{1}$$

The distribution is thus entirely specified by $p(\mathbf{u})$, the probability density function (PDF) for the displacement of a single particle.

In this paper we will study evolution from SL with the following specific PDF:[8]

$$p(\mathbf{u}) = \begin{cases} (2\Delta)^{-3} & \text{if } \mathbf{u} \in [-\Delta,\Delta]^3, \\ 0 & \text{otherwise.} \end{cases} \tag{2}$$

Each particle is therefore moved randomly in a cube of side 2Δ centered on the corresponding lattice site (Fig. 1). Taking $\Delta \to 0$, at fixed ℓ, one thus obtains a perfect lattice, while taking $\Delta \to \infty$ at fixed ℓ, one obtains an uncorrelated Poisson particle configuration [33]. Given Eq. (2), the *shuffling parameter* Δ^2 also gives the variance of the shuffling, i.e.,

$$\Delta^2 = \int d^3u u^2 p(\mathbf{u}). \tag{3}$$

Our SL configurations are therefore specified by two parameters: the lattice constant ℓ and the shuffling parameter Δ. An alternative convenient characterization is given by ℓ and the adimensional ratio $\delta \equiv \Delta/\ell$. We will refer to the latter as the *normalized shuffling parameter*. It is thus the square root of the variance of the shuffling in units of the lattice spacing.

In what follows we consider not an infinite SL, but a finite SL of N particles in a cubic box of size $L=N^{1/3}\ell$ (see Fig. 1), with periodic boundary conditions. We will consider the specific case of a *simple cubic lattice*, in which the mean number density of particles is thus $N/L^3=n_0=\ell^{-3}$. Further we will assign to all particles the same mass m, so that the average mass density is simply $\rho_0=mn_0$.

In Table I we list the various relevant parameters of the SL considered as initial conditions of the N body simulations (NBS) which we report here. We will explain below the criteria used for these choices.

B. Statistical characterization of correlation properties

The microscopic number density function for any particle distribution is given by

$$n(\mathbf{x}) = \sum_{i=1}^{N} \delta_{\mathrm{D}}(\mathbf{x}-\mathbf{x}_i), \tag{4}$$

where $\mathbf{x}_i$ is the position of the ith particle, δ_{D} is the Dirac delta function and the sum is over the N particles of the system.

[8] We will discuss in the conclusions section the importance of this specific choice for the PDF.

TABLE I. Details of the SL used as initial conditions in the simulations reported in this paper. N is the number of particles, L is the box size, ℓ the lattice constant, and Δ (δ) the (normalized) shuffling parameter. The mass m of the particles is expressed in unit of that in SL64, i.e., m_{64}. In the units chosen, the mass density in all these systems is $\rho_0=Nm/L^3=1$. Note that SL64 and SL128 are "more shuffled" than all the others (i.e., larger shuffling parameter) while SL16 is the one which is the closest to a perfect cubic lattice. Note that SL128 differs only from SL64 by the size of the box.

Name	$N^{1/3}$	L	ℓ	Δ	δ	m/m_{64}
SL64	64	1	0.015625	0.015625	1	1
SL32	32	1	0.03125	0.0553	0.177	8
SL24	24	1	0.041667	0.00359	0.0861	18.96
SL16	16	1	0.0625	0.00195	0.03125	64
SL128	128	2	0.015625	0.015625	1	1

1. The two-point correlation function

For a system such as we consider here, in which the mean density is well defined and nonzero, it is convenient to define the density contrast:

$$\delta(\mathbf{x}) = \frac{n(\mathbf{x}) - n_0}{n_0}. \tag{5}$$

In order to characterize the two-point correlation properties of the density fluctuations, one can then use the reduced two-point correlation function:

$$\tilde{\xi}(\mathbf{r}) = \langle \delta(\mathbf{x}+\mathbf{r})\delta(\mathbf{x})\rangle, \tag{6}$$

where $\langle\cdots\rangle$ is an ensemble average, i.e., an average over all possible realizations of the system. In a distribution of discrete particles $\tilde{\xi}(\mathbf{r})$ always has a Dirac delta function singularity at $\mathbf{r}=0$, which it is convenient to separate by defining $\xi(\mathbf{r})$ for $\mathbf{r}\neq\mathbf{0}$ (the "off-diagonal" part) [33]:

$$\tilde{\xi}(\mathbf{r}) = \frac{1}{n_0}\delta_D(\mathbf{r}) + \xi(\mathbf{r}). \tag{7}$$

It is useful also to note that one can write

$$\xi(r) = \frac{\langle n(r)\rangle_p}{n_0} - 1, \tag{8}$$

where $\langle n(r)\rangle_p$, the *conditional average density*, is the (ensemble) average density of points in an infinitesimal shell at distance r *from an occupied point*.[9] We will make use of this relation in estimating $\xi(r)$ below.

In the evolved self-gravitating systems we study $\xi(r)$ will invariably be a monotonically decreasing function of r. It is then natural to define a scale λ by

$$\xi(\lambda) = 1 \tag{9}$$

which separates the regime of weak correlations [i.e., $\xi(r) \ll 1$] from the regime of strong correlations [i.e., $\xi(r) \gg 1$]. In the context of gravity these are what are referred to as the *linear* and *nonlinear* regimes, as a linearized treatment of the evolution of density fluctuations is expected to be valid in the former case. Given the form of Eq. (8) it is clear that λ as defined by Eq. (9) is an appropriate definition of the *homogeneity scale* of the system. This scale gives then the typical size of strongly clustered regions.

The exact analytic expression for $\xi(r)$ in a SL is given in [25]. We do not reproduce it here as it is a complicated expression, which we will not in fact make use of. In our case, as in the case of a perfect lattice and a Poisson distribution (which, as we have noted correspond to specific limits of the SL) $\xi(r)<1$ everywhere: there is no strong clustering. In such a situation the homogeneity scale is of order of the average distance between nearest neighbors (NN), which we will denote by Λ. Thus when we refer to the homogeneity scale we will mean Λ in absence of nonlinear clustering and the scale given by Eq. (9) otherwise.

2. The mass variance

For particle distributions with a well defined average density it useful also to consider an integrated quantity such as the normalized variance of particle number (or mass) in spheres, defined as follows:

$$\sigma^2(r) = \frac{\langle N^2(r)\rangle - \langle N(r)\rangle^2}{\langle N(r)\rangle^2}, \tag{10}$$

where $N(r)$ is the number of particles in a sphere of radius r. Then $\sigma^2(r)$ can be used, in a manner similar to that described above for $\xi(r)$, to distinguish a regime of large *fluctuations* from a regime of small fluctuations. It is simple to find the explicit expression for $\sigma^2(r)$, which gives it as a double integral of $\xi(r)$ [33].

One can show that the normalized variance in real-space spheres defined in Eq. (10) behaves in a SL as $\sigma^2(r)\propto r^{-4}$ at large r, compared to $\sigma^2(r)\propto r^{-3}$ in a Poisson distribution [33,34]. The behavior $\sigma^2(r)\propto r^{-4}$ is in fact the fastest possible decay of this quantity [33]. This means that the SL belongs to the class of distributions which may be termed *superhomogeneous* [34] (or *hyperuniform* [35]). Such systems have mass fluctuations which are depressed with respect to those in an uncorrelated Poisson distribution.

3. The power spectrum

Since we consider distributions which are periodic in a cube of side L, we can write the density contrast as a Fourier series:

$$\delta(\mathbf{x}) = \frac{1}{L^3}\sum_{\mathbf{k}} \exp(i\mathbf{k}\cdot\mathbf{x})\tilde{\delta}(\mathbf{k}) \tag{11}$$

with $\mathbf{k}\in\{(2\pi/L)\mathbf{n}\,|\,\mathbf{n}\in\mathbb{Z}^3\}$. The coefficients $\tilde{\delta}(\mathbf{k})$ are given by

$$\tilde{\delta}(\mathbf{k}) = \int_{L^3} \delta(\mathbf{x})\exp(-i\mathbf{k}\cdot\mathbf{x})d^3\mathbf{x}. \tag{12}$$

The PS of a particle distribution[10] is then defined as (see, e.g., [33,36])

$$P(\mathbf{k}) = \frac{1}{L^3}\langle|\tilde{\delta}(\mathbf{k})|^2\rangle. \tag{13}$$

In distributions which are statistically homogeneous, which is the case here,[11] the PS and reduced two-point correlation function $\tilde{\xi}(\mathbf{r})$ are a Fourier conjugate pair.

[9] For the more general case of nonuniform distributions, such as fractal particle distributions [33], in which n_0 is zero, this is the basic statistical quantity for the characterization of two-point correlation properties, rather than $\tilde{\xi}(r)$ (which is then not defined).

[10] We use here the term for this quantity commonly employed in cosmology, rather than structure factor which is more habitual in the context of condensed matter and statistical physics. Note also the normalization, which corresponds to $P(\mathbf{k}\to\infty)\to\frac{1}{n_0}$, rather than unity.

[11] For the lattice and SL the ensemble average is defined over the set of lattices rigidly translated by an arbitrary vector in the unit cell.

The exact expression for the PS of a SL is simple to derive. One finds (see [33,36])

$$P(\mathbf{k}) = \frac{1-|\tilde{p}(\mathbf{k})|^2}{n_0} + L^3 \sum_{\mathbf{n}} |\tilde{p}(\mathbf{k})|^2 \delta_{\mathrm{K}}\left(\mathbf{k}, \mathbf{n}\frac{2\pi}{\ell}\right), \quad (14)$$

where $\tilde{p}(\mathbf{k})$ is the Fourier transform of the PDF for the displacements $p(\mathbf{u})$ (i.e., its characteristic function), and δ_{K} is the three-dimensional Kronecker symbol. For the specific $p(\mathbf{u})$ given in Eq. (2) we have

$$|\tilde{p}(\mathbf{k})|^2 = \prod_{i=x,y,z} \frac{\sin^2(k_i\Delta)}{(k_i\Delta)^2}. \quad (15)$$

Inserting this expression in Eq. (14) one obtains an exact explicit analytic expression for the PS of a SL in terms of the two parameters ℓ and Δ. It is simple to verify that taking $\Delta/\ell = \delta \to \infty$, at fixed ℓ, one obtains $P(k) = 1/n_0$ (as expected, since one obtains in this limit a Poisson distribution). Further one always approaches this same behavior (as required [33]) in the limit $k \to \infty$. Further, at small k (i.e., $k \ll 2\pi/\ell$), we obtain

$$P(\mathbf{k}) \approx \frac{|\mathbf{k}|^2\Delta^2}{3n_0}. \quad (16)$$

We note that this result can actually be found (see [33,36]) directly from Eq. (14), without assuming a specific form for $p(\mathbf{u})$. One need only assume that $p(\mathbf{u})$ has a finite variance, equal to Δ^2. *Thus the small k behavior of the PS of the SL does not depend on the details of the chosen PDF for the displacements, but only on its (finite) variance.*[12]

Finally note that the mass variance can actually be expressed simply as an integral in reciprocal space of the PS multiplied by an appropriately normalized Fourier transform $\tilde{W}(k;r)$ of the spherical window function, being 0 outside the sphere and 1 inside it [33]:

$$\sigma^2(r) = \frac{1}{(2\pi)^3} \int d^3k P(k) |\tilde{W}(k;r)|^2. \quad (17)$$

4. The nearest neighbor distribution

A very useful and simple statistical quantity which characterizes small-scale clustering properties of a particle distribution is the nearest neighbor (NN) PDF $\omega(r)$. It is the probability density for the distance between a particle and its NN [33], i.e., $\omega(r)dr$ gives the probability that a particle has its NN at a distance in $[r, r+dr]$. If one neglects correlations of any order higher than two, it is simple to show that $\omega(r)$ is related to the conditional density $\langle n(r)\rangle_p$ [and thus to $\xi(r)$, given Eq. (8)] through[13]

$$\omega(r)dr = \left(1 - \int_0^r \omega(s)ds\right) \cdot 4\pi r^2 \langle n(r)\rangle_p dr. \quad (18)$$

This relation will be very useful to us here because it is valid in particular when clustering is dominated, at early times, by individual pairs of particles falling toward each other.

C. Estimation of statistical quantities

In order to estimate $P(\mathbf{k})$ and $\xi(\mathbf{r})$ in a given particle configuration, i.e., in a single realization of the evolved SL, we calculate averages in spherical shells in real or reciprocal space. This means that we consider only the dependence of these quantities on the modulus of their arguments and we will therefore use the notation $P(k)$ and $\xi(r)$ in the rest of the paper.

The PS is obtained from $\tilde{\delta}(\mathbf{k})$ by means of the relation[14]

$$P(k) \approx \frac{1}{N(k)} \sum_{k \le |\mathbf{k}'| \le k+\delta k} |\tilde{\delta}(\mathbf{k}')|^2, \quad (19)$$

where $N(k)$ is simply the number of vectors $\mathbf{k}'$ considered in the sum. Note that to speed up the calculations, not all the vectors $\mathbf{k}'$ for a given modulus are taken into account: at large $\mathbf{k}$ the density of vectors considered is smaller than at small $\mathbf{k}$.

The function $\xi(r)$ is estimated by first calculating $\langle n(r)\rangle_p$ [see Eq. (8)] [33]. As already mentioned the latter gives the average density in a spherical shell of radius r, and thickness $\delta r \ll r$, centered on an occupied point. Thus we estimate it as follows:

$$\langle n(r)\rangle_p \simeq \frac{1}{V(r,\delta r)N_c} \sum_{i=1}^{N_c} N_i(r) \quad (20)$$

where $N_i(r)$ is the number of particles[15] in the spherical shell between radii r, $r+\delta r$, volume $V(r,\delta r)$, centered on the ith particle of a subset of $N_c \le N$ particles randomly chosen among the N particles of the system.

The mass variance can be simply estimated by

$$\sigma^2(r) \simeq \frac{1}{\langle N(r)\rangle^2} \frac{1}{N_c - 1} \sum_{i=1}^{N_c} (N_i(r) - \langle N(r)\rangle)^2, \quad (21)$$

where $N_i(r)$ is the number of particles contained in the ith (with $i = 1 \cdots N_c$) *randomly placed* sphere of radius r and $\langle N(r)\rangle$ its average.

Finally the NN distribution $\omega(r)$ is computed directly by pair counting.

[12] Note that the behavior $\lim_{\mathbf{k}\to\mathbf{0}} P(\mathbf{k}) = 0$ is an equivalent way of stating the property of superhomogeneity of the distribution [33].

[13] The relation follows if one assumes that the probability of finding a particle in $[r, r+dr]$ given that there is a point at $r=0$ is the same whether the condition that there be no other point in [0, r] is imposed or not.

[14] For simplicity in this paper we use the same symbol for the ensemble average quantity and for its estimator.

[15] We use periodic boundary conditions in this estimation (as in the simulations).

III. GRAVITATIONAL CLUSTERING IN A SHUFFLED LATTICE: RESULTS FROM NUMERICAL SIMULATIONS

A. Details of numerical simulations

We have performed a set of numerical simulations using the freely available code GADGET [37,38]. This code, which is based on a tree algorithm for the calculation of the force, allows one to perform simulations in an infinite space, using the Ewald summation method [39,40]. The potential used is *exactly* equal to the Newtonian potential for separations greater than the softening length ε, and regularized at smaller scales. For what concerns the integration parameter we have performed several tests to check the stability of the results at the level of numerical precision we consider in this work.[16]

We have considered as initial conditions the set of five SL described in Table I. We now explain the reasons for our choices of the parameters given.

First it is important to note that, in the limit of the pure (i.e., unsoftened) gravitational evolution of an infinite SL, there is only *one* parameter which can change the dynamical evolution nontrivially.[17] This is δ, the normalized shuffling parameter (i.e., normalized in units of the lattice spacing ℓ). Because gravity has no preferred length scale the gravitational dynamics of two infinite SL with the same δ, but different lattice spacing ℓ, can be trivially related: a rescaling of length scales is equivalent to a rescaling of time, so that the configurations of one can be mapped at any time onto the configuration of the other at a different time. The same is true for changes of the mass of the particles: two SL with the same δ, the same ℓ, but different particle masses, are related by a simple scaling of the time variable. Indeed any two SL with the same δ are strictly equivalent to one another in time if they are related to one another by any simultaneous scaling of ℓ *and* the particle mass which leaves their mass density ρ_0 fixed.

For *softened* gravity in a *finite* box, the same length scale transformations can relate trivially different SL with the same δ. In this case the relevant parameters to distinguish two SL evolved in these simulations are thus *three*, which we can take as δ, $\ell/L=N^{1/3}$, and ϵ/L.

We have chosen our (arbitrary) units of length, mass, and time as follows. Our unit of length is given by the box side of the SL64 simulation and our unit of mass by the particle mass in this same simulation. A natural choice for the unit of time is the so called *dynamical time*, defined

$$\tau_{\rm dyn} \equiv \frac{1}{\sqrt{4\pi G\rho_0}}. \tag{22}$$

As unit of time here we have made a slightly different choice of the pre-factor, with $\tau_{\rm dyn}=1.092$.[18]

In the "reference" SL64 simulation we have chosen $\delta=1$. Our choices of the parameters for the other five simulations can be understood as follows:

(i) The particle masses are chosen so that the mass density is constant. Thus the dynamical time is the same in all simulations, which is convenient for comparison, as we will see, as this is the unique time scale of these systems in the fluid limit.

(ii) The softening ε is the same in all the simulations. We have chosen $\varepsilon=0.001\,75$ in our units, which means that it is, in all the simulations, significantly smaller (at least a factor of ten) than Λ_0, the initial average distance between NN.[19]

(iii) The box size is the same in all but one simulation. This latter simulation (SL128), which is the biggest one, is used to test the accuracy with which our results are representative of the infinite volume limit (at fixed mass and particle density). Thus it is chosen to have the same parameters to SL64, differing only in its volume (which increases by a factor of 8).

(iv) For each of the four other SL simulations we change the number of particles N, which fixes ℓ. We have then chosen δ *so that the PS at small k has the same amplitude*. From Eq. (16) it it easy to see that this requires, in our chosen units,

$$\frac{\Delta^2}{n_0} \equiv \delta^2\ell^5 = (\delta^2\ell^5)_{\rm SL64} = 64^{-5}. \tag{23}$$

The PS of the SL described in Table I are shown in Fig. 2. We see, up to statistical fluctuations, that the spectra are indeed of the same amplitude at small k. Note that the Nyquist frequency $k_N=\pi/\ell$ in k space translates to the right with increasing particle number.

The particles are assigned *zero velocity* in the initial conditions (at $t=0$), and, as has been underlined, the simulations are performed in a static Euclidean universe, i.e., without expansion or nontrivial spatial curvature. We have run the simulations SL16, SL24, SL32, and SL64 up to about time 6 and the SL128 up to time 8 as for longer times the simulations begin to be dominated by a single nonlinear structure, a regime in which we are not interested since it is evidently strongly affected by finite size effects.

B. Results

In this section we analyze the results of the numerical evolution of the SL described in Table I in terms of the statistical quantities discussed above. In the first two subsections we restrict ourselves to the study of the evolution of

[16] In order to test the numerical accuracy of the simulations we have also compared the early times evolution with the prediction of the linearized treatment of the early time evolution, as described in detail in [40].

[17] By "dynamical evolution" we mean the ensemble average properties of the clustering etc. We thus suppose that this average is recovered in a single realization of an infinite volume system, i.e., that spatial ergodicity applies. The unaveraged dynamical evolution will of course vary in detail from one realization to another.

[18] This corresponds to time in units of 1000 seconds for a mass density of 1 g cm^{-3}.

[19] The smallest value of Λ_0 is that in SL64 where it is equal to $0.55/64\approx 0.0086$ as in a Poisson distribution with the same number density [33].

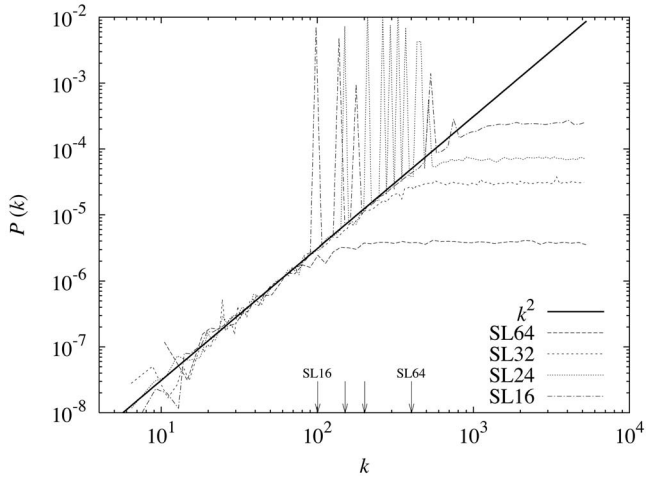

FIG. 2. The PS (averaged in spherical shells) of the SL configurations specified above in Table I as a function of the modulus of **k**. The solid line is the theoretical ($\propto k^2$) behavior for small k given by Eq. (16). At large k, the four PS are equal to $1/n_0$, with the corresponding value of n_0. The peaks arise from the second term in Eq. (14). The four arrows show the different Nyquist wave numbers multiplied by two for the SL configurations in order of increasing number density from left to right: this corresponds to the expected location of the first peak in each case. Note that, as we have discussed in Sec. II C, not all the vectors **k** are considered in the estimation of the PS and therefore only a subset of all the peaks is detected (each peak corresponds to a very narrow band of **k** so it can be easily missed).

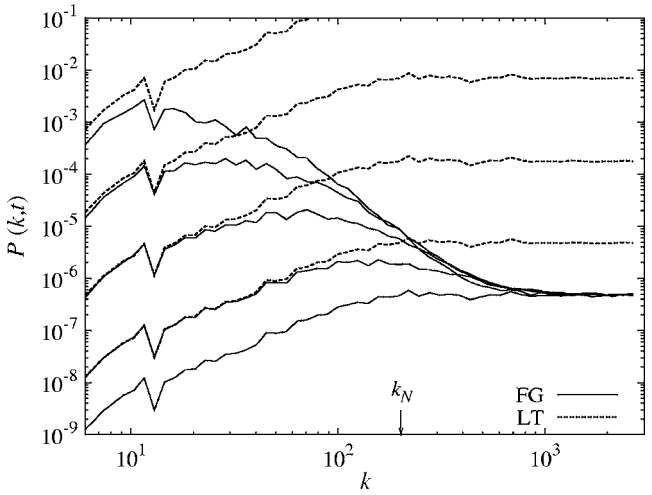

FIG. 3. Evolution of the PS in SL128 (solid lines—label FG): the curves are for time equal to 0,2,4,6,8 (from bottom to top). The dashed lines labeled with LT show the predictions of fluid linear theory, i.e., Eq. (24) with $P(k,0)$ measured in the simulation at $t=0$ for the same time steps. The arrow shows the value of the Nyquist frequency $k_N=\pi/\ell$.

SL128, i.e., the largest simulation we have run. This is then our reference point with which we compare the evolution of the other initial conditions.

1. Evolution of the power spectrum

The evolution of the PS in SL128 estimated by using Eq. (19) is shown in Fig. 3. Along with the numerical results is shown the prediction for the evolution of the PS given by the linearized fluid theory (see Appendix A):

$$P(\mathbf{k},t) = P(\mathbf{k},0)\cosh^2(t/\tau_{\rm dyn}). \tag{24}$$

We observe that:

(i) The linear theory prediction describes the evolution very accurately in a range $k<k^*(t)$, where $k^*(t)$ is a wave number which decreases as a function of time. This is precisely the qualitative behavior expected as linear theory is expected to hold only above a scale which, in real space, increases with time, and, in reciprocal space, decreases with time. We note that at $t=6$ only the very smallest k modes in the box are still in this *linear regime*, while at $t=8$ this is no longer true. We will discuss below a more precise quantification of the validity of the linearized approximation.

(ii) At very large wave numbers ($k>k_N$) the PS remains equal to its initial value $1/n_0$. This is simply a reflection of the necessary presence of shot noise fluctuations at small scales due to the particle nature of the distribution. We note that the value of k at which this behavior is attained increases somewhat from its initial value and then remains roughly stable. We will comment further on the significance of this fact below.

(iii) In the intermediate range of k, i.e., $k^*(t)<k\leq k_N$, the evolution is quite different, and *slower*, than that given by linear theory. This is the regime of *nonlinear clustering*.

These results concerning the validity of linear theory at sufficiently small k, and in a range which decreases as a function of time, are completely in line with what is observed in cosmological simulations, in an expanding universe (see, e.g., [41]). In this context simulations typically start from lattices with correlated perturbations representing spectra which are much redder than $P(k)\sim k^2$, typically $P(k)\sim k^n$ with $-3<n<0$. That the same behavior is seen in a static universe for this "bluer" PS is, however, expected. Indeed, on the basis of simple considerations (see, e.g., [16])—which do not make use of the expansion of the universe—about the long wavelength (i.e., small k) perturbations generated by nonlinear motions on small scales, one anticipates that linear theory should be valid at small k for any initial PS with $P(k)\sim k^n$ and $n<4$. The reason is that such nonlinear motions, which preserve locally mass and center of mass, can generate at most a PS at small k with the behavior $P(k)\sim k^4$.

2. Evolution of the two-point correlation function

We consider now the evolution of clustering in real space, as characterized by the reduced correlation function $\xi(r)$. We focus again on SL128. In Fig. 4 is shown the evolution of the absolute value $|\xi(r)|$ in a log-log plot. In the figure is shown also, for comparison, at large scales, the level of the typical fluctuations expected in the estimator of $\xi(r)$.[20] This indi-

[20]This estimate is obtained by assuming that the variance in the shells employed in the estimator decay as $\sqrt{\sigma^2_{\rm shell}(r)/N_c}\propto r^{-2}$, where

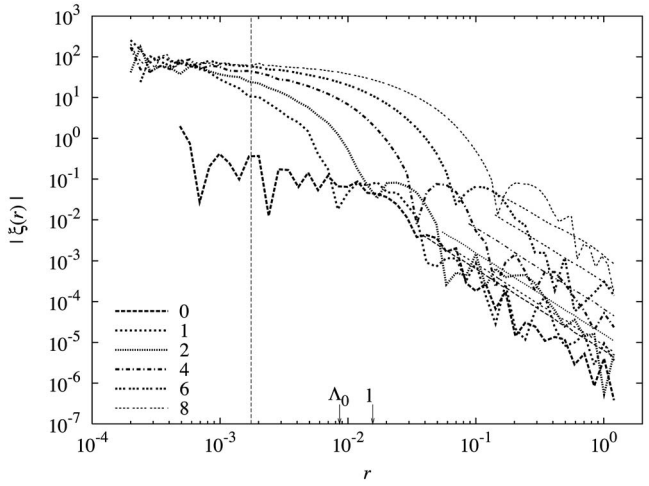

FIG. 4. Behavior of the absolute value of the correlation function $|\xi(r)|$ in SL128 at times $t=0,1,2,4,6,8$. Note that values such that $|\xi(r)|<0.01-0.1$ are below the level of noise of the estimator estimated by using the normalized variance in spherical shells (see text): This gives a limit below which the noise in the estimator dominates over the signal. The arrows show the value of the lattice spacing ℓ and the initial average distance between nearest particles Λ_0, while the dotted vertical line corresponds to the smoothing ε.

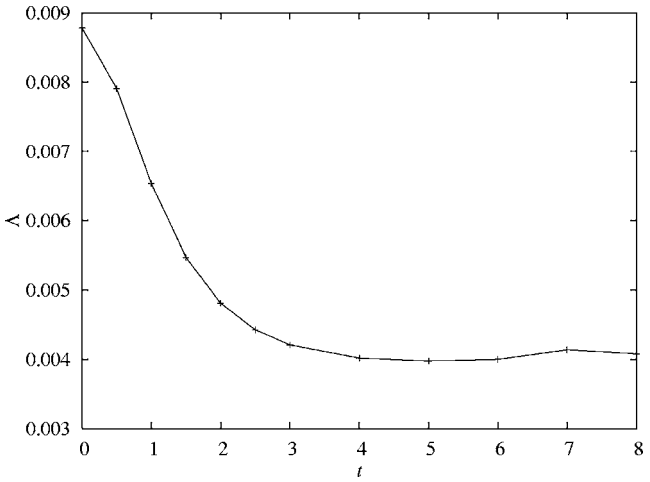

FIG. 5. Evolution in time of $\Lambda(t)$, the average distance between nearest neighbors, in SL128. It decreases at early times and then stabilizes at $\Lambda\approx 2\varepsilon$.

cates that, at larger separations, the noise in the estimator is expected to dominate over any underlying physical correlation which may be present.

We observe that: (i) Starting from $\xi(r)\lesssim 1$ everywhere, nonlinear correlations [i.e., $\xi(r)\gg 1$] develop first at scales smaller than the initial inter particle distance Λ_0. (ii) After two dynamical times the clustering develops little at scales below ε. The clustering at these scales is characterized by an approximate "plateau" at $\xi(r)\sim 10^2$. This stabilization of the system at small scales is also evident in Fig. 5, which shows the evolution of the mean distance between nearest neighbor particles as a function of time. The stabilization in time of the scale in k space at which the PS reaches its asymptotic (constant) value, which we observed above, is just the manifestation in reciprocal space of this same behavior. (iii) At scales larger than ε the correlations grow continuously in time at all scales, with the scale of nonlinearity [which can be defined, as discussed above, by $\xi(\lambda)=1$] moving to larger scales.

From Fig. 4 it appears that, once significant nonlinear correlations are formed, the evolution of the correlation function $\xi(r)$ can be described, approximately, by a simple "translation" in time. This suggests that $\xi(r,t)$ may satisfy in this regime a spatiotemporal scaling relation:

$$\xi(r,t)\approx \Xi(r/R_s(t)), \tag{25}$$

where $R_s(t)$ is a time dependent length scale which we discuss in what follows. In order to see how well such an ansatz describes the evolution, we show in Fig. 6 an appropriate "collapse plot:" $\xi(r,t)$ at different times is represented with a rescaling of the x axis by a (time dependent) factor chosen to superimpose it as closely as possible over itself at $t=1$, which is the time from which the translation appears to first become a good approximation. We can conclude clearly from Fig. 6 that the relation (25) indeed describes very well the evolution, down to separations of order ε, and up to scales at which the noise dominates the estimator.

In Fig. 7 is shown the evolution of the rescaling factor $R_s(t)$ found in constructing Fig. 6, as a function of time, with the (arbitrary) choice $R_s(1)=1$. Shown in Fig. 7 are also three (theoretical) curves, which we will explain in the next subsection. Before this we remark on two further aspects of the scaling relation which are worth noting: (i) The function $\Xi(r)$, when it is larger than ~ 0.1, can be well approximated by a simple power law with an exponential cutoff:

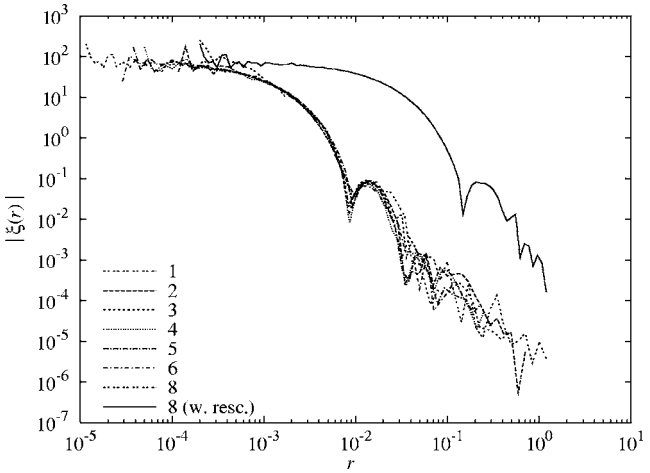

FIG. 6. Collapse plot of $\xi(r,t)$: for each time $t>1$ we have rescaled the x axis by a time-dependent factor to collapse all the curves (dashed ones) to that at time $t=1$. We have added for comparison $\xi(r,t=8)$ without rescaling ("w. resc.," continuous line).

$\sigma^2_{\text{shell}}(r)$ is the variance in shells, defined analogously to that in spheres [cf. Eq. (10)], and N_c is the number of centers used to calculate $\xi(r)$ [cf. Eq. (20)].

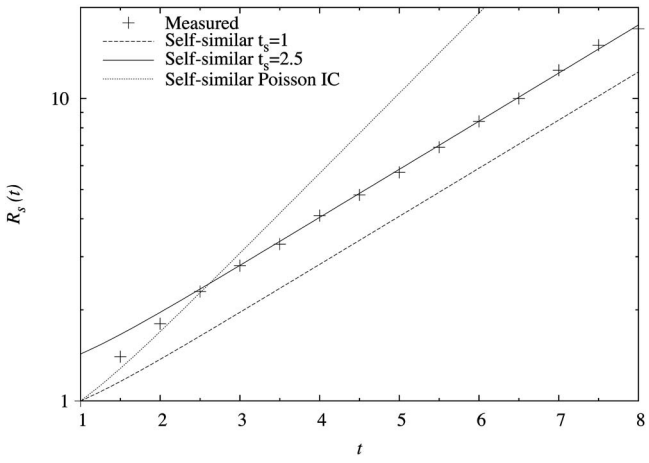

FIG. 7. Evolution of the function $R_s(t)$ in SL128 (crosses) compared with its prediction for different values of the time scale of onset of self-similarity (see text for details). Both lines correspond to $R_s(t) \propto \exp[(2/5)t/\tau_{\rm dyn}]$. Also shown is the corresponding prediction for Poisson initial conditions, $R_s(t) \propto \exp[(2/3)t/\tau_{\rm dyn}]$.

$$\Xi(r) \approx A\left(\frac{r}{\hat{R}}\right)^{-\gamma} \exp\left(-\frac{r}{\hat{R}}\right), \tag{26}$$

where we have estimated (see Fig. 8) the following values for the three parameters: $A=40$, $\gamma=0.28$, and $\hat{R}=1.45 \times 10^{-3}$. This last parameter gives the normalization of $\xi(r,t)$ at $t=1$. In order to see how well this fit describes the evolution, we show in Fig. 8 both the data and the curves inferred from it, using $R_s(t)$ as measured.

(ii) Since we have defined the homogeneity scale λ by $\xi(\lambda)=1$ it is clear that, once the spatiotemporal scaling relation is valid, we have $\lambda(t) \propto R_s(t)$.

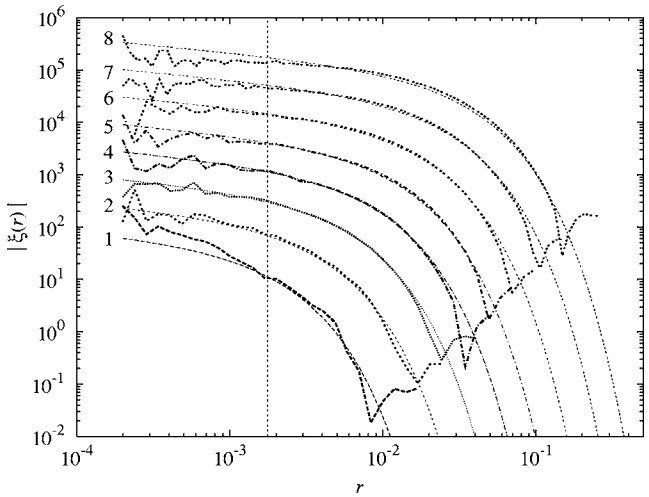

FIG. 8. Comparison of $\xi(r,t)$ measured in SL128 with the formula in Eq. (26), using the rescaling of Eq. (25). For clarity the amplitudes of the different curves have been rescaled (by a factor 3^{t-1}). Moreover, for all the curves, we have plotted only the scales such that $\xi(r,t) \gtrsim 0.1$ since Eq. (26) does not describe smaller amplitude correlations. The vertical line corresponds to the softening length ε.

(iii) Since the PS and mass variance are simply related to $\xi(r)$, we expect the scaling relation to be reflected in one for these quantities as well. We will see to what extent this is the case below.

3. Spatiotemporal scaling and "self-similarity"

We have observed that, from $t \sim \tau_{\rm dyn}$, the two-point correlation function, at least down to $\xi(r) \sim 0.01$ (level of estimator noise) obeys to a good approximation the spatiotemporal scaling relation Eq. (25), with the measured $R_s(t)$ shown in Fig. 7. In this section we discuss this result, in particular its relation to similar behaviors which have been studied in cosmology.

In the context of cosmological N body simulations this kind of behavior, *when $R_s(t)$ is itself a power law (in time)*, is referred to as *self-similarity*. Such behavior is expected in an evolving self-gravitating system (see, e.g., [16,21,32]) because of the scale-free nature of gravity, *if* the expanding universe model *and* the initial conditions *contain no characteristic scales*. Initial conditions in N-body simulations do, however, necessarily contain one such scale, which is associated to the particle discreteness (i.e., the grid spacing ℓ in the case of a perturbed lattice). Further, as we have discussed above, simulations introduce (at least) two further scales: the box-size L and force softening ε. Thus self-similarity is expected to be observed in N body simulations of an Einstein-de Sitter model (i.e., a flat matter dominated universe), starting from pure power-law initial PS $P(k) \sim k^n$, *if all effects associated with these length scales can be neglected*.

On theoretical grounds there are different expectations ([21,32,42]) about the range of exponents n of the PS which should give self-similar behavior. Effects coming from the particle discreteness are expected to become less important as the PS becomes redder (i.e., smaller n, with more relative power at larger scales), while a PS which is too "red" will become sensitive to finite size effects (i.e., to the box size). A more quantitative analysis of the dependence of dynamically relevant quantities (e.g., the variance of velocity and force fields) on these ultraviolet and infrared cutoffs suggests that self-similarity should apply in the range $-1 < n < +1$, and such behavior has in fact been observed, to a good approximation, to apply in simulations in an EdS universe of such spectra [21,22]. While there has been considerable discussion also of the case $-3 < n < -1$ in the literature, with different conclusions about the observed degree of self-similarity, the case $n \geqslant 1$ has remained open.[21] In our discussion below we will see in greater detail why the cases $n > 1$ and $n < 1$ are expected to be possibly very different with respect to self-similarity.

Our results above clearly suggest that what we have observed is a simple generalization of this self-similarity to a

[21]The reason why the case $n > 1$ has not been studied numerically appears to be twofold: first, it is not of direct interest to "real" cosmological models which typically describe PS with exponents in the range $-3 < n < -1$; secondly, the evolution from such initial conditions is considered "hard to simulate" (see, e.g., [22]).

static universe (in which there is evidently also no characteristic length scale), and to the case $n=2$. Let us examine more carefully whether this is the case, by generalizing to the static case the argument (see, e.g., [16]) used to derive the power-law behavior of $R_s(t)$ in an expanding universe.

In order to derive this behavior of $R_s(t)$, we *assume* that the spatiotemporal scaling relation holds exactly, i.e., *at all scales*, from, say, a time $t_s>0$. For $t>t_s$ we have then

$$\begin{aligned} P(\mathbf{k},t) &= \int_{L^3} \exp(-i\mathbf{k}\cdot\mathbf{r})\xi(\mathbf{r},t)d^3\mathbf{r} \\ &= R_s^3(t)\int_{L^3} \exp[-iR_s(t)\mathbf{k}\cdot\mathbf{x}]\Xi(|\mathbf{x}|)d^3\mathbf{x} \\ &= R_s^3(t)P(R_s(t)\mathbf{k},t_s), \end{aligned} \tag{27}$$

where we have chosen $R_s(t_s)=1$. Assuming now that the PS at small k is amplified as given by linear theory, i.e., as in Eq. (24), one infers for any PS $P(k)\sim k^n$ (and $n<4$ so that linear theory applies):

$$R_s(t) = \left(\frac{\cosh\dfrac{t}{\tau_{\rm dyn}}}{\cosh\dfrac{t_s}{\tau_{\rm dyn}}}\right)^{2/(3+n)} \xrightarrow{t\gg t_s} \exp\left[\frac{2(t-t_s)}{(3+n)\tau_{\rm dyn}}\right]. \tag{28}$$

In the asymptotic behavior the relative rescaling in space for any two times becomes a function only of the *difference* in time between them so that we can write

$$\xi(r,t+\Delta t) = \xi\left(\frac{r}{R_s(\Delta t)},t\right); \quad R_s(\Delta t) = e^{2\Delta t/(3+n)\tau_{\rm dyn}}. \tag{29}$$

This is analogous to what is called self-similarity in EdS cosmology. In that case the linear theory describes a growing and a decaying mode, both of them power laws in time. Asymptotically $R_s(t)$ is thus itself a simple power law.[22]

Let us now return to Fig. 7. In addition to the measured values of $R_s(t)$ the figure shows two curves corresponding to Eq. (28) with $n=2$. The first corresponds to taking $t_s=1$ in the derivation above, i.e., assuming that the scaling relation holds at all scales for $t>1$. The second is the same functional behavior, but rescaled by a constant to give a good fit to the larger time (from $t>t_s\sim 2.5$) behavior. This latter behavior is clearly very consistent with the relation given in Eq. (28): starting from this time the slope is very close to constant and equal to $\frac{2}{5}$ in units of $\tau_{\rm dyn}$.

Our results are thus indeed clearly well interpreted as a generalization in a static universe of self-similarity as observed in simulations EdS universes, for redder spectra. This self-similarity sets in, however, from about $t_s=2.5$, while we observed the spatiotemporal scaling relation already to apply approximately from $t\sim 1$ ($\approx\tau_{\rm dyn}$). Note that the fact that the functional behavior of $R_s(t)$ in $1<t<2.5$ is inconsistent with Eq. (28) with $n=2$ *implies* that the spatiotemporal scaling relation cannot hold at all scales at these times: specifically it cannot hold at small k, where $P(k)\propto k^2$, as we have seen that at these scales the PS *is* linearly amplified at this time.

A possible explanation for this behavior is suggested by the third curve (labeled "Poisson") shown in Fig. 7. This curve corresponds to Eq. (28) with $n=0$ and $t_s=1$. The fact that it fits the points reasonably well—although not so well as the $n=2$ theoretical curve for $t>2.5$—suggests the following interpretation: between $1<t<2.5$ we are observing a first phase of self-similarity, restricted to smaller scales, where the initial PS is roughly flat (i.e., Poisson-like with $n=0$) in a small range of k around the Nyquist frequency (see Fig. 3). Such an interpretation is consistent with the fact that the $\xi(r)$ in the nonlinear regime observed in simulations from Poissonian initial conditions is, to a very good approximation, the same as that observed from SL initial conditions [29,43]. On the other hand, the wave modes at which the PS is Poisson-like are very large—of the order of the inverse of the interparticle spacing—and so the observation of apparent self-similarity driven by these fluctuations is somewhat surprising: such behavior is expected, as we have discussed above, when the effects of discreteness may be neglected. We will see below that this interpretation of the spatiotemporal scaling observed in the correlation function at nonlinear scales at early times—as a first phase of self-similarity driven by Poisson fluctuations at small scales—is not correct. In particular it is reproduced in the smaller simulations we will analyze below in which there is no initial Poisson plateau around k_N.

4. Evolution of the mass variance

In this section we study the normalized mass variance $\sigma^2(r)$, defined in Eq. (10). Through the study of this quantity we can probe further the scaling properties (and self-similarity) we have just seen. We can also explain and see the interesting and nontrivial differences in this respect between the case of a power law PS with $n<1$ and $n>1$.

Given that the mass variance is expressible [cf. Eq. (17)] as an integral of the PS, one might anticipate that it will show, at large r, the same behavior as the PS at small k, i.e., we expect to find the simple scale independent amplification of linear theory:

$$\sigma^2(r,t) = A_{\sigma^2}(t)\sigma^2(r,0) \tag{30}$$

where

$$A_{\sigma^2}(t) = \cosh^2(t/\tau_{\rm dyn}) \propto R_s^{3+n}(t) \tag{31}$$

for a PS $P(k)\propto k^n$ at small k.

In Fig. 9 is shown the temporal evolution in SL128 of $\sigma^2(r)$. At each time we observe at large r the behavior $\sigma^2(r)\propto 1/r^4$ characteristic of a SL. The dotted lines show the best fit to the behavior of Eq. (30) above, which we find is

$$A_{\sigma^2}(t) = \cosh^{8/5}(t/\tau_{\rm dyn}) \propto R_s^4(t), \tag{32}$$

rather than the anticipated behavior of Eq. (31) for $n=2$.

[22] One has [16,21] $P(k,t)\propto t^{4/3}k^n$ at small k, and thus $R_s(t)\propto t^{4/3(3+n)}$.

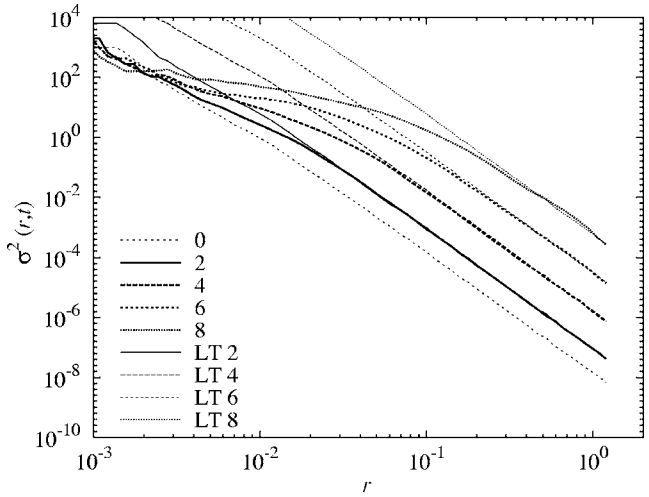

FIG. 9. Evolution of the mass variance in SL128 at times $t=0,2,4,6,8$, together with the predictions of Eq. (32) (labeled as LT).

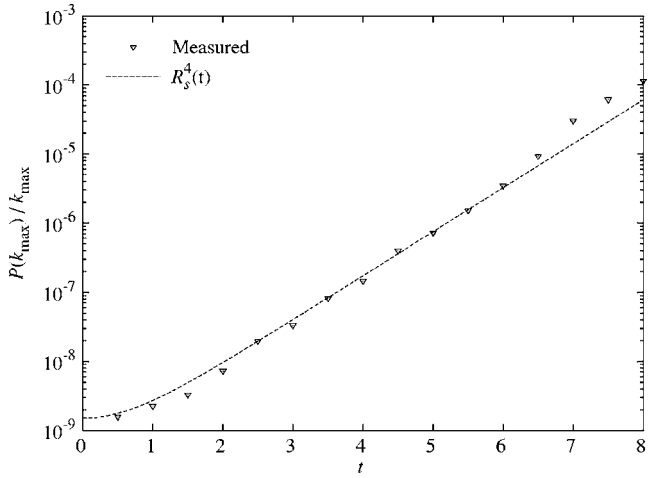

FIG. 10. Behavior of $P(k_{\max},t)/k_{\max}$ as a function of time measured in SL128. The dashed line represents the behavior given in Eq. (35).

The reason for this discrepancy is, as we now discuss, very simple. It is of importance as it makes explicit the difference between the cases of PS with $n<1$ and $n>1$. Indeed examining the integral Eq. (17) in closer detail it turns out that there is a qualitatively different behavior in the two cases. For $-3<n<+1$ the integral is dominated by modes $k\sim r^{-1}$ and one has

$$\sigma^2(r,t) \approx Ck^3P(k,t) \tag{33}$$

where $k=1/r$ and C is a constant pre-factor which depends on n. From this it follows that linear amplification of the PS at small k gives linear amplification of the mass variance at large scales. For $n>1$, however, the integral in Eq. (17) with $P(k)\sim k^n$ at all k diverges, and an ultraviolet cutoff k_c above which $P(k)/k$ decays to zero is required to regulate it.[23] The effect of the cutoff is to give

$$\sigma^2(r) \sim k_c^{-1}P(k_c)/r^4$$

at sufficiently large r. Thus, for $n>1$ the evolution of the mass variance at large r (and thus at small amplitude) is sensitive to the evolution of the cutoff in the PS (and the amplitude of the PS at this cutoff). From Fig. 3 we expect that in our system the role of k_c will be played by $k_{\max}(t)$, the wave number at which the PS reaches its maximum, and so we will have, at large r,

$$\sigma^2(r,t) \sim \frac{k_{\max}^{-1}(t)P(k_{\max},t)}{r^4}. \tag{34}$$

From Fig. 3 we see that $k_{\max}$ is clearly in the range in which the amplification in k space is nonlinear. Thus the evolution of this quantity, even at very large scales, is determined by modes in k space which are in the nonlinear regime. Given the time evolution we have observed for $\sigma^2(r,t)$ in Fig. 9, we must have

$$k_{\max}^{-1}(t)P(k_{\max},t) \sim R_s^4(t). \tag{35}$$

In Fig. 10 we see that this behavior is indeed well approximated. It is in fact evidently the direct consequence of the self-similarity as it is reflected in the variance, and, equivalently, in k space. To the extent that both quantities approximate the self-similarity observed in $\xi(r,t)$, any length scale derived from either the variance or PS must scale $\propto R_s(t)$. Thus, in particular, $k_{\max}^{-1}\propto R_s(t)$ and the maximum value of the PS, which has dimensions of volume, must scale as $P(k_{\max},t)\propto R_s^3(t)$ in this regime.

It is instructive also to examine a little further how the spatiotemporal scaling behavior, and self-similarity, are approximated in the variance. In order to illustrate this we consider the temporal evolution of scales $\lambda(\alpha,t)$ defined by the relation

$$\sigma^2(\lambda(\alpha,t),t) = \alpha, \tag{36}$$

where α is a chosen constant. If there is a spatiotemporal scaling in the system we should find that $\lambda(\alpha,t)\propto R_s(t)$. In particular any choice $\alpha\sim 1$ gives, as we discussed in Sec. II, a reasonable definition for the homogeneity scale, which should be equivalent to the one we have taken above [$\xi(\lambda,t)=1$ once nonlinear clustering has developed]. In Fig. 11 we show $\lambda(\alpha,t)$ for $\alpha=20,10,1,0.1$; also shown are curves proportional to $R_s(t)$ in the self-similar regime [i.e., as given by Eq. (28) with $n=2$]. The figure illustrates nicely how the scaling applies only at large scales (corresponding to smaller fluctuations) initially and then propagates to smaller (more nonlinear) scales. At the time $t\approx 2.5$, which we identified above in our analysis of $\xi(r,t)$ as the time from which self-similarity is well approximated, the scaling behavior given by $R_s(t)$ is manifestly well approximated for $\alpha\gg 1$, i.e., into the nonlinear regime. We do not, however, see a behavior consistent with the hypothesis that the evolution prior to this time $(1<t<2.5)$ is self-similar and associated to a PS

[23] Such a cutoff necessarily exists in any particle distribution as $P(k)$ cannot diverge for large k. One necessarily has, as we have discussed, $P(k)\to 1/n_0$ for $k\to\infty$ [33].

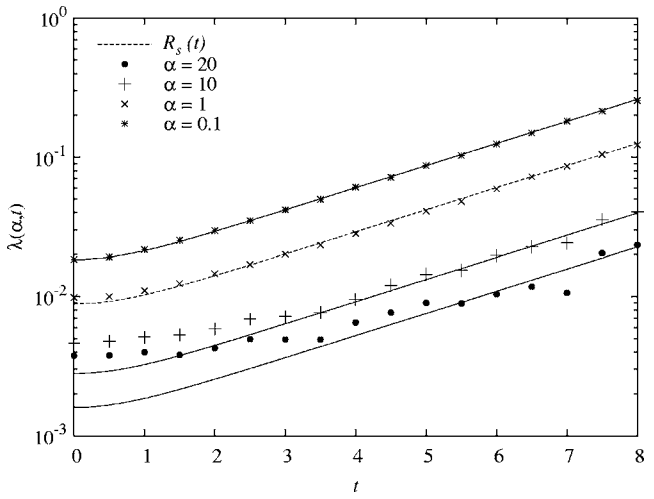

FIG. 11. Behavior of $\lambda(\alpha,t)$, the length for which $\sigma^2(r,t)=\alpha$ for $\alpha=0.1,1.0,10.0,20.0$ in the simulations SL128.

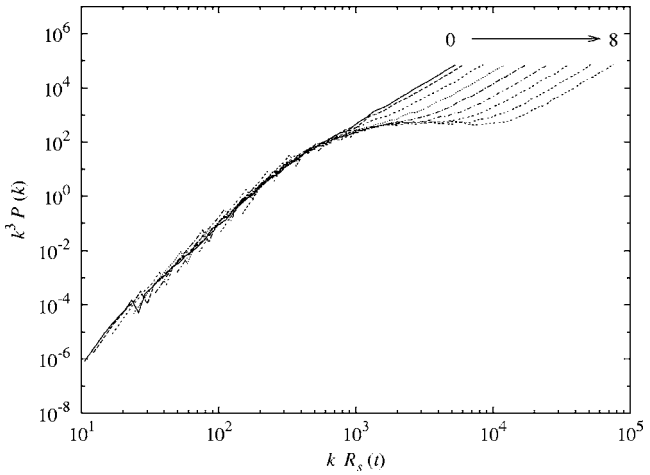

FIG. 12. Collapse plot of $\Delta^2(k,t)$ for the SL128 simulation using as scaling factor $R_s(t)$ as described in Eq. (37).

with $n=0$ around k_N: this would correspond as in Fig. 7 to a faster evolution of the scales shown here at these times, which is not what is observed.

5. Self-similarity and the regime of validity of linear theory

The derivation of $R_s(t)$ in Eq. (28) explains implicitly the physical origin of the self-similar behavior: if the small k PS is a simple power law, the evolution of the two-point correlation function is self-similar, with $R_s(t)$ given by Eq. (28), in the approximation that fluctuations grow as described by the linearized fluid theory. Self-similarity applies to the full evolution to the extent that this self-similar temporal evolution at linear scales becomes "imprinted" on smaller nonlinear scales. The mechanism by which this happens is simply the collapse of the initial mass fluctuations at large scales, at time scales fixed by linear theory. Self-similarity is thus a good approximation to the extent that the clustering amplitudes at any scale depend only on the prior history of larger scales. In terms of power transfer in the evolution of clustering, self-similarity can thus be interpreted qualitatively as indicating that there is a much more efficient transfer of power from large to small scales than in the opposite direction. Our results here show that this is true also in more "blue" initial conditions with a small k PS $P(k)\propto k^n$ and $n>1$, in which the variance of mass in real space spheres is dominated by fluctuations at much smaller scales which evolve in the nonlinear regime.

These points are further illustrated in Fig. 12, which shows a "collapse plot" for the temporal evolution of $\Delta^2(k,t)\equiv k^3P(k)$. It follows from Eq. (27) that, when self-similarity applies, we have the behavior

$$\Delta^2(k,t)=\Delta^2(R_s(t)k,t_s), \tag{37}$$

where, as above, $t_s<t$ is an arbitrary initial time and $R_s(t)$ is given by Eq. (28). In Fig. 12 is plotted the rescaled function at each time, starting from $t_s=0$. At small k, we see that right from the initial time the self-similarity is indeed followed (as the rescaled curves are always superimposed at these scales). This is simply because linear theory, which is valid at these scales, gives such a behavior. As time progresses we see the range of k in which the curves are superimposed increases extending into the nonlinear regime. Thus the self-similarity "propagates" progressively from small k to larger k, carried by the scales which are evolving nonlinearly. Note that the behavior at asymptotically large k is simply $\Delta^2(k,t)\propto k^3/n_0$ (where n_0 is the mean particle density) at all times, corresponding to the shot noise present in all particle distributions with average density n_0 and which by definition does not evolve in time.[24]

Let us finally return to the question of the breakdown of linear theory. In our discussion of Fig. 3 in Sec. III B 1 above, we noted that the scale-independent amplification of linear theory describes very well the evolution of the PS up to wave number k, which we denoted $k_*(t)$ and which decreases with time. A question of interest is what the criterion is which determines this scale, i.e., what the criterion is for the application of linear theory. We cannot answer this question rigorously without considering, at least, the next order in this perturbative treatment.[25] We will not attempt to do so here, but rather consider determining such a criterion phenomenologically (i.e., from the simulations).

In principle this criterion may, in general, be quite complicated, as it would be expected to depend on the fluctuations present at all scales. Once we are in the self-similar regime, however, we expect that all characteristic scales in k space, and in particular $k_*(t)$, should scale $\propto R_s^{-1}(t)$. Such a time dependence results if one supposes $k_*(t)$ determined by

[24]Note that in the two-point correlation function this time independent discrete contribution appears as a singularity at the origin. It therefore does not "pollute" the collapse plots for $\xi(r,t)$. This also explains why one is able to identify the scaling behavior more readily by eye in this quantity. The collapse plot for $\sigma^2(r,t)$, which we have not shown, is similar to that for $\Delta^2(k)$.

[25]It is in fact possible [16] to write the equation for the evolution of density fluctuations in k space in a convenient form for this purpose, with all corrections to the linearized fluid limit in two formally simple terms. See also [3] for discussion of these issues.

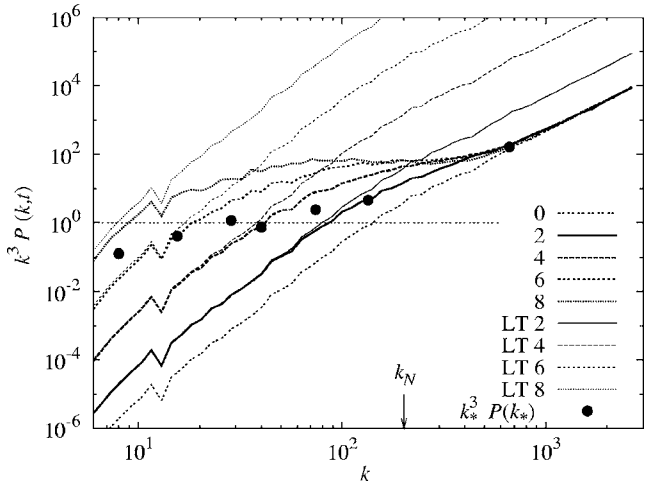

FIG. 13. Behavior of $\Delta^2(k,t)$ in SL128 together with the prediction of linear theory (LT). The points correspond to the value of $\Delta^2(k_*,t)$, at times (from right to left) 1, 2, 3, 4, 5, 6, and 7, where k_* is the wave number above which the evolution of the PS is no longer well approximated by linear theory.

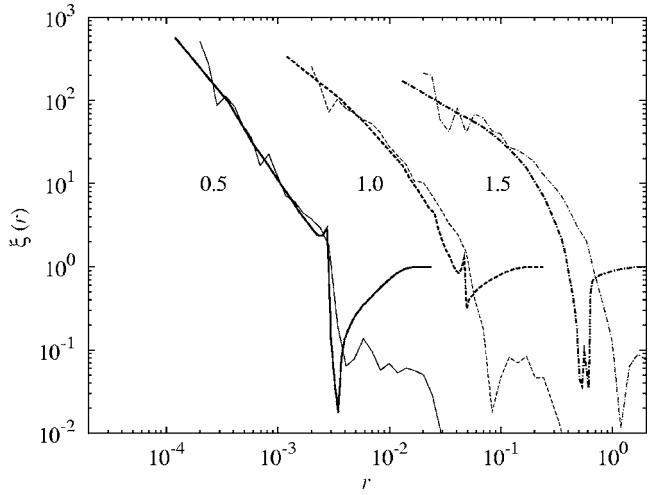

FIG. 14. Two-point correlation function in SL128 at times $t=0.5,1,1.5$ (thin lines) together with the approximation obtained from the NN PDF (thick lines). For clarity the behaviors at different times have been arbitrarily rescaled on the x axis.

a dimensionless quantity having some given amplitude. The evident simple criterion which suggests itself is

$$\Delta^2(k_*(t),t) = \text{constant}. \tag{38}$$

Figure 13 shows the evolution of $\Delta^2(k,t)$, together with the evolution in linear theory. The points (small black circles) mark the approximate value of k_* at each time, determined as the scale at which the full evolution deviates from the linear theory in each case.[26] The horizontal line shows that, starting from about $t=3$, when the self-similarity has set in, Eq. (38) with the constant set equal to unity is a reasonably good fit to the observed $k_*(t)$. The deviation of the last point, at $t=7$ can be attributed to finite size effects, as we see that at this time the smallest k modes in the box are no longer described well by the linear evolution.

For $n<1$, because of Eq. (33), the criterion Eq. (38) for the breakdown of linear theory is equivalent to one stating it as a threshold value of the real space variance. In the current case, with $n>1$, there is no such evident equivalence, as the mass variance at scales $r>k_*^{-1}(t)$ are not directly determined by the fluctuation of these modes, but rather by the fluctuations in larger k modes. Thus in this case the physical criterion for the breakdown of linear theory is really more appropriately given in k space.[27]

[26]The value of k_* in Fig. 13 (used for the points) has been estimated using the following criterion: $|\ln P(k_*,t)/\ln P_{\rm LT}(k_*,t)-1| = 0.05$, where $P_{\rm LT}(k,t)$ is simply the initial PS amplified by linear theory, i.e., Eq. (24).

[27]If one wishes to define a real-space scale directly, this can be done by using the mass variance defined in a Gaussian window, i.e., with $\tilde{W}(k;r)$ in Eq. (17) given by a Gaussian of width $1/r$. This is really just a trivial way of restating the k space condition in real space.

6. Role of two-body correlations

The gravitational force on a particle in an SL is dominated, for small δ, by that exerted by its six nearest neighbors, and for large δ, by its single nearest neighbor [25]. One thus expects that, at sufficiently early times, the dynamical evolution should be well approximated by neglecting all but these dominant contributions to the force. It has in fact been shown in [29] that the early time evolution of simulations of small δ SL can be well approximated by a two phase model: in a first phase the particle moves under the effect of its six nearest neighbors, and then subsequently, when the lattice symmetry is broken, under the effect only of a single nearest neighbor. The first nonlinear correlations then emerge as these nearest neighbor pairs fall toward one another.

As described in Sec. II the relation Eq. (18) holds in the approximation that the correlations are primarily due to correlated pairs of nearest neighbor particles. Its validity is thus a good probe of the probable adequacy of a dynamical model like that just described. In Fig. 14 is shown the comparison of the two relevant quantities: the correlation function measured in the simulation and the one reconstructed by using Eq. (18), i.e., by considering explicitly only nearest neighbors (NN) correlations. We see that the relation holds very well until $t=1$.

This is a quite striking and surprising result: the form of $\xi(r,t)$—which is subsequently that which is observed to scale in the asymptotic self-similar evolution—has already emerged at a time when nearest neighbor interactions play a crucial role in the dynamics. In the previous sections, however, we have seen that this asymptotic behavior is characterized by a time dependence derived in a fluid limit. Such a limit is normally expected to be valid in the opposite case that two or few body interaction with nearest neighbor particles can be neglected (rather than being dominant in the approximation just considered). While we note that when the asymptotic scaling behavior is not necessarily explicitly

dependent on the characteristic length scales in the system—notably those associated with the discreteness of the distribution which directly enter in determining the strength of nearest neighboring forces. We will discuss this point further below after a presentation of results of the other SL simulations we have performed.

7. Dependence on the normalized shuffling parameter

As discussed above SL initial conditions may be characterized, for their gravitational evolution, by the single dimensionless parameter δ. Our analysis until now has concerned solely the simulation SL128 and thus only a single value ($\delta=1$). Our primary result—that this system tends in a few dynamical times to a self-similar evolution—would be expected to be true for any (finite) value of δ: this particular spatiotemporal scaling behavior is determined solely by the k^2 *form* of the small k PS, which is invariant under changes in δ. Thus the only thing that we would expect to change nontrivially when δ changes is the transient regime to the asymptotic self-similar behavior. Specifically we might expect both the duration of this transient and its nature to change.

The emergence of self-similarity in the evolution corresponds, as we have discussed at length, to a behavior which is explicitly independent of the discreteness scale ℓ characterizing its particlelike nature. The simplest interpretation of this behavior—and the usual one in cosmology—is that this corresponds to a fluidlike behavior of the system, i.e., to an evolution which can be described, at both linear and nonlinear scales, by a set of nonlinear fluid equations approximating the particle dynamics.[28] If this interpretation is correct, any δ-dependent effects in the evolution of SL with different δ, but with the *same* large scale fluctuations (i.e., small k PS) can then be considered as "discreteness effects."

This equivalence of the fluid limit of the evolution from SL with different δ can be seen even more explicitly as follows, for the case that δ is small. In this limit the so-called Zeldovich approximation to the fluid limit evolution (see Appendix B below) is valid. Each element of the fluid then moves according to

$$\mathbf{x}(\mathbf{q},t) = \mathbf{q} + f(t)\mathbf{u}(\mathbf{q},t=0), \tag{39}$$

where $\mathbf{q}$ is a Lagrangian (time-independent) coordinate, which we can take here to be the lattice point from which the particle/fluid element is displaced, and $\mathbf{u}(\mathbf{q},t=0)$ is the displacement of the particle/fluid element at the initial time. The function $f(t)$ is simply the growth factor of the fluctuations in linear theory. The effect of the evolution, in this limit, is thus manifestly to transform one SL into another one with a different (larger) δ. Thus in the linear fluid limit, starting from a small δ, the evolution of the system should be *identical* (statistically, and up to an overall scale transformation) to that of an SL with a larger δ.

The simulations SL64, SL32, SL24, and SL16, as we have defined them allow us to explore the δ dependence (and thus nonfluid effects) in the evolution from SL initial conditions. As described above in Sec. II, we have chosen in each case a combination of δ and ℓ which leaves the amplitude of the PS constant (in the length units we have chosen, fixed by the box size in these simulations). This choice means that the evolution of any two simulations in time should agree (without any rescaling) if the evolution of both may be well described by the fluid limit: this is governed, as we have seen, by the evolution of the fluctuations at large scales which are identical.

These statements are of course true in the approximation that effects introduced by the finite box-size of the simulation, the softening of the force and any other effects of the numerical discretization of the evolution, are negligible. We noted that in a *finite* box, and with *softened* gravity, one has *two* additional parameters, which one can choose as ℓ/L and ε/L. The simulations SL64, SL32, SL24, and SL16 in Table I correspond, as we have described, to chosen *fixed* values of these two parameters. In order to control for dependence on the box size L, we have chosen SL64 to have the same δ as SL128, so that the two sets of initial conditions differ only in the box size. Thus these two simulations should give precisely the same (averaged) results as long as finite size effects play no significant role. We will not report in this paper the sensitivity of results to the choice of ε. We have, however, verified that, for a considerable range of variation of ε to smaller values than the one used in the simulations we report here, there is no notable effect on our results in the range of scales $r > \varepsilon$ where we assume them to be valid.

In Fig. 15 are shown $\xi(r,t)$ in each of the five SL simulations given in Table I, for different times, starting from $t=1$ when the structures first develop in the largest simulations until $t=6$ when the scale of homogeneity has reached a significant fraction of the box size.

The first point to note is the excellent agreement between the results of SL128 and SL64, which differ only in the size of the simulation box. This assures us that the finite size effects due to the different values of L, up to the time we have shown, are very small in the SL64 simulation, and we will assume the same is true for the SL32, SL24, SL16 simulations (in ascribing the differences between them solely to the change in δ and not to that in the number of particles).

Considering now the evolution of the other simulations we observe that:

(i) As δ decreases the time increases at which the system begins to evolve and form strong nonlinear correlations [i.e., develop a region with $\xi(r,t) \gg 1$]. This is a qualitative behavior expected also in the fluid limit: in the Zeldovich approximation Eq. (39) the displacements grow at a rate given by the function $f(t)$ which is independent of scale. Thus, starting

[28] More precisely the system is assumed then to evolve as described by a set of Vlasov-Poisson equations. See appendices below.

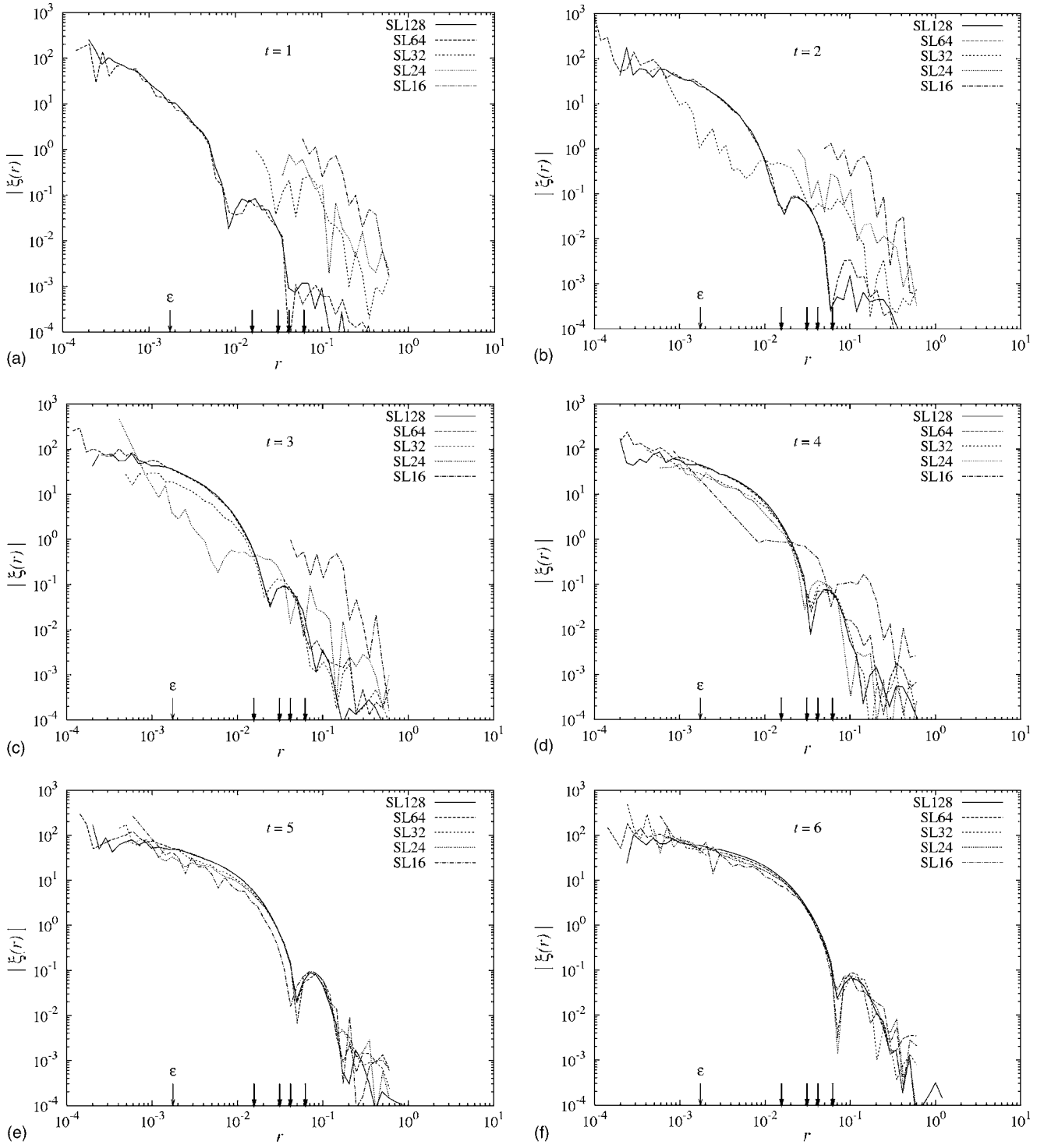

FIG. 15. Evolution of the two-point correlation function in the different simulations at times 1, 2, 3, 4, 5, and, 6. The four thick arrows represent the different mesh sizes ℓ while the thin one corresponds to the value of the softening length ε.

from a smaller δ, the time at which nonlinear structures form (when $\delta \sim 1$) is necessarily longer.[29]

(ii) When the first nonlinear correlations develop there is a manifest δ dependence in the correlation functions, i.e., the correlations are not (statistically) equivalent to those in the larger δ simulations. This means that at the time these correlations emerge, the smaller δ system is not evolving as in its fluid limit. If it were it would be in agreement with the

[29]Equivalently one can say that the larger l system is "missing input power" above its Nyquist frequency compared to the smaller l simulation.

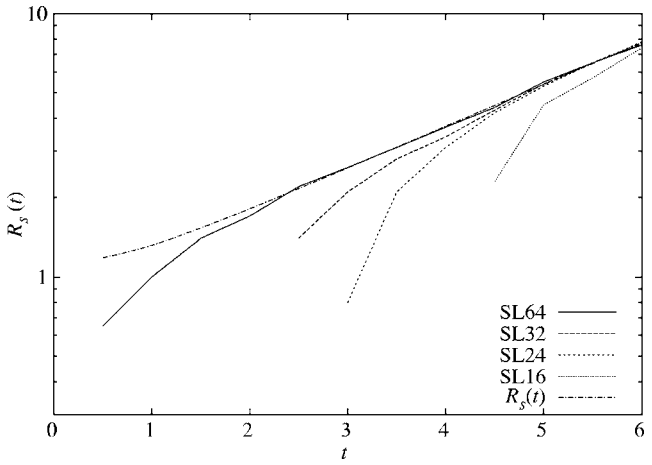

FIG. 16. Evolution of the rescaling factor $R_s(t)$ in the different simulations. Also shown is the self-similar behavior Eq. (28).

larger δ simulation with the same initial power at the relevant scales.

(iii) Initially the nonlinear correlations formed in each system "lag behind" those in the larger δ simulation, i.e., $\xi(r,t)$ typically has a smaller amplitude in the smaller δ simulations. As it evolves the smaller δ system eventually "catches up" with the larger ones, its correlations eventually agreeing very well with those in all the larger δ systems over a significant range of scale.

(iv) The *form* of the nonlinear correlation function in the asymptotic regime—the self-similar regime we have discussed above—emerges to a very good approximation at a time when there is still a quite visible lag in amplitude.

In Fig. 16 we show also the evolution of $R_s(t)$, inferred in each case, as in our analysis of SL128 above, by the determination of the factor which describes the spatiotemporal scaling once it emerges as a good approximation. We observe that in each case we have, as for SL128, a regime of approximate spatiotemporal scaling of the nonlinear correlation function *before* the asymptotic selfsimilar regime is reached. In this regime $R_s(t)$ is smaller in amplitude than in the asymptotic regime, corresponding to the lag of the smaller δ simulations described. However, $R_s(t)$ evolves more rapidly than in the asymptotic regime, allowing each system to catch up with the δ-independent behavior. Note that these observations again confirm that the corresponding regime in $R_s(t)$ in SL128 should indeed not be ascribed to a first self-similar phase driven by the Poisson fluctuations present in this case.

Both this lagging and the role of nearest neighbor interactions in the formation of the first structures can be explained in the framework of a refined version of the "two phase model" of [29] for the early time correlations. We will present this model in detail elsewhere, and restrict ourselves here to a few qualitative comments.

A very good approximation to the evolution of a perturbed lattice is provided by a perturbative treatment described in [40,44]. The force acting on particles is written as an expansion in the relative displacement of particles, in a manner completely analogous to a standard technique used in solid state physics to treat perturbations to crystals. One can then do a linear mode analysis in k space to determine the eigenmodes of the displacement fields under gravity. While at small k one recovers the simple k-independent amplification of linear fluid theory, the effect at larger k (i.e., $k \sim k_N$) is, for all but some very specific modes, to slow down the growth of fluctuations. Thus the "collapse time" for fluctuations at scales of order of the interparticle distance are indeed slowed down, as observed here, compared to linear fluid theory.

This approximation to the early time evolution breaks down when the force on a particle starts to be dominated by a single nearest neighbor. At this point particles start to accelerate toward their neighbor, giving rise to strong two-body correlations which are, as we have seen above, the dominant contribution to the measured two-point correlations at nonlinear scales at early times. We have remarked that, given this manifestly "nonfluid" mechanism for the formation of these correlations, it is somewhat surprising to see approximately the same two-point correlations maintained in the "self-similar" regime, if this regime is interpreted as the result of a purely fluidlike evolution. Two possible, but very different, explanations for this are the following:

(i) The self-similar evolution of the system in the nonlinear regime is not correctly interpreted as a manifestation of a purely fluid limit of the N body system. Its time scales are dictated by the fluid limit (giving the collapse time for fluctuations at large scales), but its nonlinear dynamics are intrinsically discrete;

(ii) The early time nonlinear correlations, well described by a discrete dynamics, approximate well those in the fluid limit because the nonlinear fluid dynamics is in fact physically well approximated by a discrete system, i.e., the nonlinear evolution of the fluid, in the relevant phase of moderately strong nonlinear correlations ($\xi(r) < 10^2$), is well described as the evolution of "lumps" of fluid toward "nearest neighbor lumps."

We will evaluate these two quite different interpretations of our results more quantitatively in future work.

IV. DISCUSSION AND CONCLUSIONS

To conclude we first summarize our results, and then make a few remarks on open questions to be explored in further works.

We have studied the evolution under their Newtonian self-gravity, in a static Euclidean space, of classical point particles initially distributed in *infinite* space in a quasiuniform manner. This is a paradigmatic problem of the out of equilibrium statistical mechanics of long range interacting systems, which has received little attention in this context. Specifically we have considered a one relevant parameter class of initial conditions in which the particles are randomly perturbed off a lattice. We have found that our simulations converge aysmptotically (but for times smaller than those at which the size of the finite simulation box becomes relevant) to solutions characterized by a simple spatiotemporal scaling relation in which the temporal dependence of the scaling can be derived from the linearized fluid theory. These results are qualitatively very similar to those observed in numerical studies in the context of cosmology, i.e., for expanding

spacetimes and for more complex initial conditions in which the displacements of the particles off the lattice are correlated in order to produce the PS of fluctuations of cosmological models. More specifically, the observed spatiotemporal scaling is a simple generalization of what is known in the cosmology literature as self-similarity in an expanding universe to the case of (i) a static universe, and (ii) a PS $P(k) \propto k^2$. Further we have observed that there is a transient phase to this behavior, in which already, to a good approximation, the same spatiotemporal scaling relation holds for the two-point correlation function $\xi(r,t)$, but with a more rapid temporal evolution of the scaling factor. We have noted that the lagging of the evolution behind the asymptotic behavior in this regime can be ascribed to effects of discreteness (i.e., nonfluid effects) slowing down the evolution of fluctuations at scales comparable to the interparticle distance which have been quantified in [40,44]. We have seen also that the form of the correlation function emerges already at the very early times when the first nonlinear correlations develop due to two-body correlations which develop under the effect of nearest neighbor interactions.

The gravitational evolution of a SL in a static universe thus shares the qualitative features of similar, but more complicated models, in cosmology. It thus provides a simplified "toy model" in which to study some fundamental problems which remain open concerning the evolution of these systems, which have been studied extensively in numerical simulations but remain poorly understood analytically, notably:

(i) The absence of a theory which adequately explains the shape (i.e., functional form) and evolution of the observed nonlinear correlations.

(ii) The absence of a "theory of discreteness errors." In cosmology simulations of particles displaced off lattices (or "glasses") aim to reproduce the evolution of a self-gravitating fluid. There is currently very little systematic understanding of how well this evolution is actually approximated. We have highlighted in this paper that the SL gives a very well defined, and simplified, framework in which to address this problem.

Let us remark finally on a few other points:

(i) We have worked here with initial velocities set equal to zero. In exploring the analogy with cosmological simulations there is another choice of initial velocities which is natural. This is that given by the Zeldovich approximation discussed above, with $f(t)$ chosen in Eq. (39) to correspond to the purely growing mode of density fluctuations, i.e., $f(t) = e^{t/\tau_{\rm dyn}}$. The initial velocities are then simply the initial displacements divided by $\tau_{\rm dyn}$. This introduces no further new characteristic scales in the initial conditions. Its effect on the evolution will be to make the transient to self-similarity slightly shorter, but it will not significantly change any of our findings or conclusions.

(ii) We have made a specific choice of PDF for our shuffling, given in Eq. (2). We expect different choices again to modify slightly the nature of the transient, but not the self-similarity. This latter, as we have emphasized, depends only on the k^2 form of the PS at small k, which is in fact the same for any PDF with finite variance. Indeed the coefficient of the k^2 is just given by this variance, and the difference between PDFs will manifest themselves in modifications of the fluctuations at small scales (i.e., larger k). For example if the two PDF have different fourth moments, this will be reflected in a different coefficient in the k^4 correction to the small k PS. Just as in the case of velocities, there is a natural choice if one wishes to maximize the analogy with cosmological simulations: a simple Gaussian PDF which is what is used in this context. In fact this choice is also natural from another point of view (see [45] for a detailed discussion): when one considers constructing new particle distributions by a simple "coarse-graining" on some scale, the SL with Gaussian PDF, due to the central limit theorem, has the property of being the unique one which is invariant under such a coarse graining.

(iii) We have reported in this paper simulations in which the softening ε has been kept fixed (in our chosen length units). We have mentioned that we have checked that our results for clustering amplitudes above this scale are robust to the use of significantly smaller values of ε. A more extensive and systematic study of the role of this parameter would, however, be of interest, specifically with the goal of understanding in detail how the clustering properties are modified by it at small scales.

ACKNOWLEDGMENTS

We thank the "Centro Ricerche e Studi E. Fermi" (Roma) for the use of a supercomputer for numerical calculations, the EC Grant No. 517588 "Statistical Physics for Cosmic Structures" and the MIUR-PRIN05 project on "Dynamics and thermodynamics of systems with long range interactions" for financial support. M. J. thanks the Istituto dei Sistemi Complessi for its kind hospitality during October 2005 and May 2006. We are indebted to B. Marcos for extensive collaboration on closely related work.

APPENDIX A: FLUID EQUATIONS AND FLUID LINEAR THEORY

The equations which describe the evolution of a self-gravitating fluid are the following (e.g., [16], Chap. II or [24], Chap. 5.2):

$$\partial_t \rho + \nabla_{\mathbf{x}} \cdot (\rho \mathbf{v}) = 0, \tag{A1a}$$

$$\partial_t \mathbf{v} + (\mathbf{v} \cdot \nabla_{\mathbf{x}})\mathbf{v} = \mathbf{g} - \frac{1}{\rho}\nabla_{\mathbf{x}} p, \tag{A1b}$$

$$\nabla_{\mathbf{x}} \cdot \mathbf{g} = -4\pi G(\rho - \rho_0), \tag{A1c}$$

$$\nabla_{\mathbf{x}} \times \mathbf{g} = 0, \tag{A1d}$$

where $\rho(\mathbf{x},t)$ is the mass density, $\mathbf{v}(\mathbf{x},t)$ the velocity field, $\mathbf{g}(\mathbf{x},t)$ the gravitational field, and $p(\mathbf{x},t)$ the pressure. The set of equations closes if $p(\mathbf{x},t)$ is specified as a function of the density.

As it is shown in [16,19], this set of equations can be obtained after certain approximations from the Vlasov equation coupled to the Poisson equation:

$$[\partial_t + \mathbf{v}\cdot\boldsymbol{\nabla}_{\mathbf{x}} - \boldsymbol{\nabla}_{\mathbf{v}}\Phi\cdot\boldsymbol{\nabla}_{\mathbf{v}}]f(\mathbf{x},\mathbf{v},t) = 0, \tag{A2a}$$

where Φ satisfies the modified Poisson equation

$$\boldsymbol{\nabla}_{\mathbf{x}}^2\Phi(\mathbf{x},t) = 4\pi G\left[m\int_{\mathbb{R}^3} f(\mathbf{x},\mathbf{v},\mathbf{t})d^3\mathbf{v} - \rho_0\right] \tag{A2b}$$

and $f(\mathbf{x},\mathbf{v},t)$ is the density of particles in the infinitesimal volume $d^3\mathbf{x}d^3\mathbf{v}$ at $(\mathbf{x},\mathbf{v})$ at time t. These equations can themselves be derived as truncations of a Born-Bogoliubov-Green-Kirkwood-Yvon hierarchy [16,19], or starting from a Liouville equation for the full ("spiky") one particle phase space density [46,47].

By performing a perturbation analysis for the case of pressureless (i.e., highly nonrelativistic or "cold") matter, around $\rho=\rho_0$ and $\mathbf{v}=\mathbf{0}$ with the set of Eq. (A1), one finds at first order that the evolution of the density contrast $\delta(\mathbf{x},t) = (\rho-\rho_0)/\rho_0$ is described by the differential equation

$$\ddot{\delta}(\mathbf{x},t) = 4\pi G\rho_0\delta(\mathbf{x},t) \tag{A3}$$

or equivalently that each Fourier mode $\tilde{\delta}(\mathbf{k},t)$ evolves independently of the others:

$$\ddot{\tilde{\delta}}(\mathbf{k},t) = 4\pi G\rho_0\tilde{\delta}(\mathbf{k},t). \tag{A4}$$

The general solution of Eq. (A3) is ([16], Sec. 13)

$$\delta(\mathbf{x},t) = A(\mathbf{x})(\sqrt{4\pi G\rho_0}t) + B(\mathbf{x})\exp(-\sqrt{4\pi G\rho_0}t). \tag{A5}$$

For the case, as in this paper, in which the initial velocity is set equal to zero, one obtains

$$\delta(\mathbf{x},t) = \delta(\mathbf{x},0)\cosh(\sqrt{4\pi G\rho_0}t). \tag{A6}$$

APPENCIX B: LAGRANGIAN FLUID THEORY AND THE ZELDOVICH APPROXIMATION

The previous appendix uses the Eulerian formalism of fluid mechanics, in which one describes the evolution of the different quantities characterizing the fluid (velocity, density, and pressure) at each point of a fixed reference frame. In the alternative Lagrangian formalism (see, e.g., [48–50]), one describes the evolution of the fluid in terms of the displacements of its elements with respect to a reference frame. In that case, the equations (A1) which describe the density and the velocity are then transformed into a set of equations describing the evolution of a displacement field $\mathbf{f}(\mathbf{X},t)$. The position $\mathbf{x}$ of a fluid element at time t is then written

$$\mathbf{x} = \mathbf{f}(\mathbf{X},t), \tag{B1}$$

where the coordinate $\mathbf{X}$ labels the fluid element considered. One can choose this coordinate as the position of the fluid element at the initial time (which we assume to be 0): $\mathbf{X}=\mathbf{f}(\mathbf{X},0)$. The equations for $\mathbf{f}(\mathbf{X},t)$ in the case of a gravitating fluid can be found in, e.g., [49]. Note that in this reference, a fluid in an expanding universe is considered. The static case can be recovered by setting the expansion factor $a(t)=1$ at all times.

As in the Eulerian approach, one can perform a perturbation theory in the Lagrangian approach. One writes $\mathbf{f}(\mathbf{X},t) = \mathbf{X}+\mathbf{p}(\mathbf{X},t)$ with $\mathbf{p}(\mathbf{X},0)=\mathbf{0}$, and performs a Taylor expansion in powers of $\mathbf{p}$. At linear order in $\mathbf{p}(\mathbf{X},t)$, one obtains the following set of equations:

$$\boldsymbol{\nabla}\cdot(\ddot{\mathbf{p}} - 4\pi G\rho_0\mathbf{p}) = -4\pi G\rho_0\delta(\mathbf{X},0), \tag{B2}$$

$$\boldsymbol{\nabla}\times\ddot{\mathbf{p}} = \mathbf{0}, \tag{B3}$$

where $\delta(\mathbf{X},0)$ is the density contrast at $t=0$. Writing the vector field $\mathbf{p}$ as the sum of a curl-free part $\mathbf{p}_D$ and a divergenceless part $\mathbf{p}_R$ (i.e., $\mathbf{p}_D$ can be written as the gradient of a scalar function, and $\mathbf{p}_R$ as the curl of a vector field), one finds after some calculation that

$$\mathbf{p}(\mathbf{X},t) = \ddot{\mathbf{p}}(\mathbf{X},0)\frac{[\cosh(\sqrt{4\pi G\rho_0}t)-1]}{4\pi G\rho_0} + \dot{\mathbf{p}}_D(\mathbf{X},0)\frac{\sinh(\sqrt{4\pi G\rho_0}t)}{\sqrt{4\pi G\rho_0}} + \dot{\mathbf{p}}_R(\mathbf{X},0)t \tag{B4}$$

with the initial condition $\mathbf{p}(\mathbf{X},0)=\mathbf{0}$. Note that $\ddot{\mathbf{p}}(\mathbf{X},0) = \ddot{\mathbf{p}}_D(\mathbf{X},0)$ since the gravitational force is conservative. This Eq. (B4) corresponds to Eqs. (6) and (7) in [49], with $a(t)=1$ and $\Lambda=4\pi G\rho_0$.

The asymptotic behavior of the solution (B4) is

$$\mathbf{p}(\mathbf{X},t) \xrightarrow[t\to\infty]{} \frac{1}{2}\left[\frac{\ddot{\mathbf{p}}(\mathbf{X},0)}{4\pi G\rho_0} + \frac{\dot{\mathbf{p}}_D(\mathbf{X},0)}{\sqrt{4\pi G\rho_0}}\right]\exp(\sqrt{4\pi G\rho_0}t). \tag{B5}$$

By choosing $\dot{\mathbf{p}}_R(\mathbf{X},0)=\mathbf{0}$ and $\ddot{\mathbf{p}}(\mathbf{X},0)\sqrt{4\pi G\rho_0}=\dot{\mathbf{p}}(\mathbf{X},0)$, the solution is then directly in its asymptotic regime. This is the static space equivalent of the Zeldovich approximation in an expanding background [49–52].

The linear approximation of the Lagrangian approach, which leads to the Zeldovich approximation as we have described, has proven to be very useful in the problem of gravitational clustering. With respect to the linear Eulerian approach, it has the advantage that it can describe the evolution of density fluctuations with a density contrast much greater than unity.

[1] Y. Elskens, M. K.-H. Kiessling, and V. Ricci, e-print math-ph/0506078.
[2] *Dynamics and Thermodynamics of Systems with Long-Range Interactions*, edited by T. Dauxois, S. Ruffo, E. Arimondo, and M. Wilkens (Springer, Berlin, 2002).
[3] T. Padmanabhan, Phys. Rep. **188**, 285 (1990).
[4] C. H. Reick, Phys. Rev. E **66**, 036103 (2002).
[5] I. Ispolatov and E. G. D. Cohen, Phys. Rev. E **64**, 056103 (2001).
[6] O. Iguchi, Y. Sota, A. Nakamichi, and M. Morikawa, Phys. Rev. E **73**, 046112 (2006).
[7] O. Iguchi, Y. Sota, T. Tatekawa, A. Nakamichi, and M. Morikawa, Phys. Rev. E **71**, 016102 (2005).
[8] H. de Vega and N. S'anchez, Nucl. Phys. **B625**, 409 (2002).
[9] H. de Vega and N. S'anchez, Nucl. Phys. **B625**, 460 (2002).
[10] P.-H. Chavanis, Physica A **361**, 55 (2006).
[11] K. R. Yawn, B. N. Miller, and W. Maier, Phys. Rev. E **52**, 3390 (1995).
[12] B. N. Miller, Phys. Rev. E **53**, R4279 (1996).
[13] K. R. Yawn and B. N. Miller, Phys. Rev. Lett. **79**, 3561 (1997).
[14] K. Yawn and B. N. Miller, Phys. Rev. E **56**, 2429 (1997).
[15] T. Tatekawa, F. Bouchet, T. Dauxois, and S. Ruffo, Phys. Rev. E **71**, 056111 (2005).
[16] P. J. E. Peebles, *The Large-Scale Structure of the Universe* (Princeton University Press, Princeton, 1980).
[17] T. Padmanabhan, *Structure Formation in the Universe* (Cambridge University Press, Cambridge, 1995).
[18] D. Daley and D. Vere-Jones, *An Introduction to the Theory of Point Processes* (Springer-Verlag, Berlin, 1988).
[19] W. Saslaw, *The Distribution of the Galaxies* (Cambridge University Press, Cambridge, 2000).
[20] O. Iguchi, T. Kurokawa, M. Morikawa, A. Nakamichi, Y. Sota, T. Tatekawa, and K.-i. Maeda, Phys. Lett. A **260**, 4 (1999).
[21] G. Efstathiou, C. S. Frenk, S. D. M. White, and M. Davis, Mon. Not. R. Astron. Soc. **235**, 715 (1988).
[22] R. E. Smith, J. A. Peacock, A. Jenkins, S. D. M. White, C. S. Frenk, F. R. Pearce, P. A. Thomas, G. Efstathiou, and H. M. P. Couchman, Mon. Not. R. Astron. Soc. **341**, 1311 (2003).
[23] K. Huang, *Statistical Mechanics* (Wiley, New York, 1988).
[24] J. Binney and S. Tremaine, *Galactic Dynamics* (Princeton University Press, Princeton, 1994).
[25] A. Gabrielli, T. Baertschiger, M. Joyce, B. Marcos, and F. Sylos Labini, Phys. Rev. E **74**, 021110 (2006).
[26] M. K.-H. Kiessling, Adv. Appl. Math. **31**, 132 (2003).
[27] M. Bottaccio, A. Amici, P. Miocchi, R. Capuzzo Dolcetta, M. Monturori, and L. Pietronero, Europhys. Lett. **57**, 315 (2002).
[28] M. Bottaccio, L. Pietronero, A. Amici, P. Miocchi, R. Capuzzo Dolcetta, and M. Montuori, Physica A **305**, 247 (2002).
[29] T. Baertschiger and F. Sylos Labini, Phys. Rev. D **69**, 123001 (2004).
[30] W. C. Saslaw, Astrophys. J. **341**, 588 (1989).
[31] G. Efstathiou, M. Davis, C. S. Frenk, and S. D. M. White, **57**, 241 (1985).
[32] B. Jain and E. Bertschinger, Astrophys. J. **456**, 43 (1996).
[33] A. Gabrielli, F. Sylos Labini, M. Joyce, and L. Pietronero, *Statistical Physics for Cosmic Structures* (Springer, Berlin, 2004).
[34] A. Gabrielli, M. Joyce, and F. Sylos Labini, Phys. Rev. D **65**, 083523 (2002).
[35] S. Torquato, *Random Heterogeneous Materials* (Springer, New York, 2001).
[36] A. Gabrielli, Phys. Rev. E **70**, 066131 (2004).
[37] www.mpa-garching.mpg.de/galform/gadget/index.shtml.
[38] V. Springel, N. Yoshida, and S. D. M. White, New Astron. Rev. **6**, 79 (2001) (also available on [37]).
[39] L. Hernquist, F. R. Bouchet, and Y. Suto, Astrophys. J. **75**, 231 (1991).
[40] B. Marcos, T. Baertschiger, M. Joyce, A. Gabrielli, and F. Sylos Labini, Phys. Rev. D **73**, 103507 (2006).
[41] R. H. Miller, Astrophys. J. **270**, 390 (1983).
[42] B. Jain and E. Bertschinger, Astrophys. J. **509**, 517 (1998).
[43] T. Baertschiger, M. Joyce, and F. Sylos Labini, Astrophys. J. **581**, L63 (2002).
[44] M. Joyce, B. Marcos, A. Gabrielli, T. Baertschiger, and F. Sylos Labini, Phys. Rev. Lett. **95**, 011304 (2005).
[45] T. Baertschiger, M. Joyce, A. Gabrielli, and F. Sylos Labini, e-print cond-mat/0612594.
[46] T. Buchert and A. Knebe, Astron. Astrophys. **438**, 443 (2005).
[47] H. Spohn, *Large Scale Dynamics of Interacting Particles* (Springer-Verlag, Berlin, 1991).
[48] J. Ehlers and T. Buchert, Gen. Relativ. Gravit. **29**, 733 (1997).
[49] T. Buchert, Mon. Not. R. Astron. Soc. **254**, 729 (1992).
[50] V. Sahni and P. Coles, Phys. Rep. **262**, 1 (1995).
[51] Y. B. Zeldovich, Astron. & Astroph., pp. 84–89 (1970).
[52] S. F. Shandarin and Y. B. Zeldovich, Rev. Mod. Phys. **61**, 185 (1989).